Preprint
UCRL-JC-143047

Industrial Applications of Low Temperature Plasmas

J.N. Bardsley

This article was submitted to
DisplaySearch Conference, Austin, Texas, March 20-22, 2001

March 15, 2001

U.S. Department of Energy

Lawrence
Livermore
National
Laboratory

Industrial Applications of Low Temperature Plasmas

J. Norman Bardsley

Lawrence Livermore National Laboratory
and the
United States Display Consortium

Abstract. The use of low temperature plasmas in industry is illustrated by the discussion of four applications, to lighting, displays, semiconductor manufacturing and pollution control. The type of plasma required for each application is described and typical materials are identified. The need to understand radical formation, ionization and metastable excitation within the discharge and the importance of surface reactions are stressed.

INTRODUCTION

Gaseous discharges have been used in industry for over a century, beginning well before the discovery of the electron and the consequent understanding of the mechanisms by which charge is separated and transported in gases. The important early empirical progress included the discovery of arc lamps by Davy around 1801, with application to lighting in mines, and of the dielectric barrier discharge in 1857 by Siemens (1), which led to the efficient production of ozone.

Until the discovery of the transistor and the development of integrated circuits, the use of ionized gases was essential to the control of electric currents within the electrical power and communications industries, creating the interdisciplinary field known as gaseous electronics. Although most of the gaseous (often inappropriately called "vacuum") components within electronic systems disappeared with the development of semiconductor technology, the manufacture of semiconductor devices is dependent upon the use of gas discharges through plasma processing techniques. Meanwhile, understanding of ionized gases is still essential to the lighting and display industries, despite the advent of light emitting diodes, solid-state lasers and liquid crystal displays.

This paper will not attempt a comprehensive review of all industrial applications of low temperature plasmas. The focus will be on four areas, lighting, electronic displays, semiconductor manufacturing and pollution control. These four industries are at very different stages of evolution and thus have varying ability to support research.

The lighting industry is relatively mature. For mass-produced lamps, approximately 75% of the global market is held by three multinational companies, the pace of technological evolution is relatively slow and profit margins are thin. More companies are involved in producing specialty lighting products, and the opportunities for innovation and double-digit profit margins are greater.

The display industry is at a very exciting stage, in that the dominance of the cathode ray tube is being challenged by flat panel display (FPD) technologies. There is a great need for research, but most of the manufacturing activity is concentrated in Asia. Furthermore, although the global FPD industry has invested over $20B in fabrication facilities during the last ten years, this investment has yet to produce any sustained profits.

The semiconductor industry is now dependent on plasma processes for the production of devices with sub-micron features. The manufacture of plasma reactors has become a large international industry, with annual revenues in excess of $10B. The business is still extremely volatile. As this article was being written, during the early weeks of 1998, several leading U. S. suppliers of semiconductor manufacturing equipment curtailed operations in response to the financial problems in Asia, but by the time that this volume reaches the reader, the expansion may have resumed.

The use of plasma techniques in pollution control has received much attention in recent years. Although ozonizers have been long used for water treatment and electrostatic precipitators for dust control, most of the newer methods have not yet been accepted commercially. The two most important remaining challenges are to reduce the cost of manufacture and operation of the equipment and to be able to guarantee that no harmful by-products are created as the target pollutants are destroyed.

Even within the restricted scope of this review, much more good work has been done than can be reported in the space available. The selection of references is somewhat arbitrary, and apologies are extended to those authors whose work is not acknowledged in this brief report.

LIGHTING

This section will provide brief descriptions of the operation of several of the most common lamps. In the first two examples, electrons and ions play minor roles, but the interaction between a heated gas and the various surface materials is critical to the performance of the lamp.

There are three major characteristics that are used in comparing the performance of different lamps, efficiency, color characteristic and lifetime. Other essential factors that constrain lamp design are size, shape, safety in both fabrication and use, and environmental impact. By far the most important consideration is cost. For almost all application cost constraints rule out many technological options and cost minimization within traditional designs is critical in maintaining market leadership.

Lamp efficiency is a measure of the apparent brightness of the light (in lumens) produced for each watt of electrical power. The lumen unit allows for the wavelength dependent response of the human eye. The efficiency of the nominal eye in the blue (450 nm), green (555 nm) and red (610 nm) is 51.5, 683 and 343 lumens per radiant watt, respectively. The theoretical efficiency of a three-wavelength emission source with acceptable color rendering is approximately 300 lumen per watt (lpw).

The efficiency of commonly used lamps rose substantially between 1940 and 1980, as shown in Figure 1, but has risen little since that time. The most efficient commercial sources with acceptable color mix are the fluorescent and metal halide lamps, which have an efficiency just over 100 lpw, a figure which has changed little over the past twenty years. The sodium lamp produces about 20% more useful light, but with poor color balance.

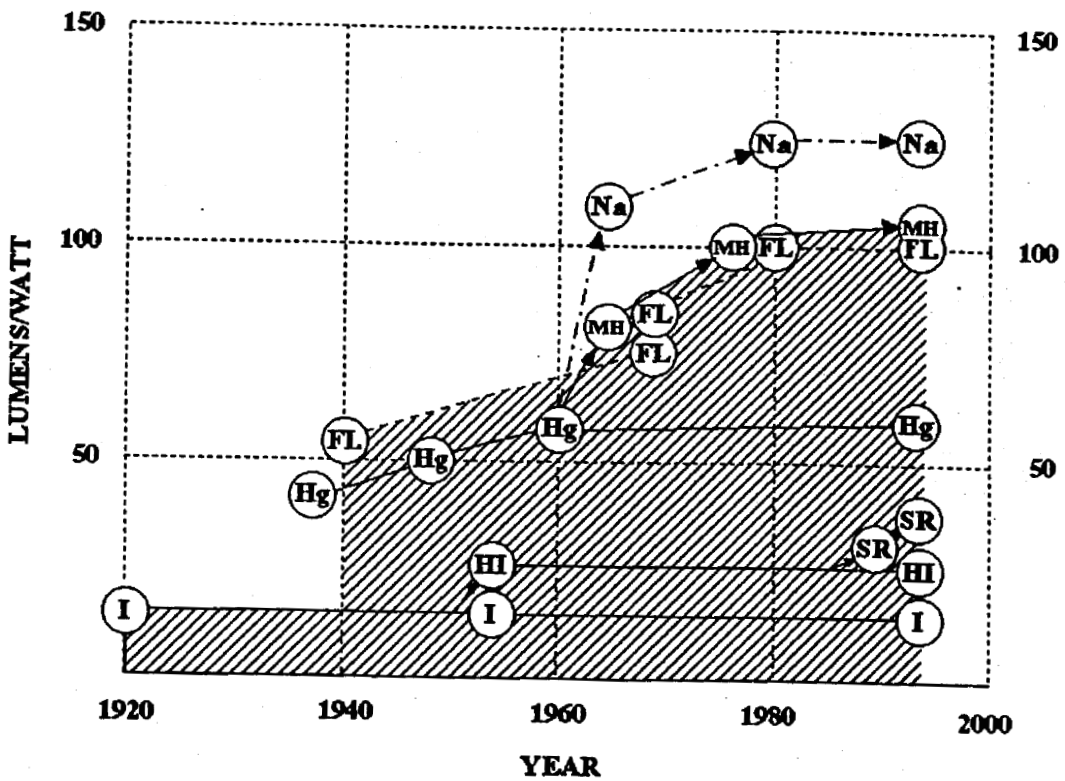

FIGURE 1. The evolution the efficiency of lamp technology since 1920: I, incandescent; HI halogen -cycle incandescent; SR, same with IR reflector; Hg, high-pressure mercury lamp for street-lighting; FL, fluorescent, MH, metal-halide lamp; Na, high pressure sodium arc lamp (Courtesy: J. F. Waymouth).

Color balance can be achieved using a continuous spectrum, such as black-body radiation at a temperature around 5500K. However, such high temperatures are difficult to sustain in compact lamps without going to high pressures. Alternatively, one can use a mix of discrete sources distributed across the visible spectrum. The

desired emission frequencies can be produced either through direct excitation of visible transitions, or through the creation and down-conversion of UV light.

Lamp lifetime is determined mainly by the stability of the various surfaces exposed to the radiation and fill gases. Particular care has to be taken to avoid the growth of hot spots in which damage grows exponentially. For example, localized evaporation from incandescent filaments can increase the resistance, leading to more heating and enhanced evaporation. Deleterious heating can also be caused by deposition of opaque material on the glass envelope of the lamp.

Incandescent Lamps

In incandescent lamps, light is produced by radiation from a heated filament. Although the first commercial incandescent lamps of Edison and others used carbon filaments, tungsten has been the material of choice for the last forty years, because of a combination of three properties. With a melting temperature close to 3650K, tungsten has the lowest evaporation rate of all natural metals. Its emission spectrum enhances the production of visible light by about 30% over that of a black-body source. Finally, tungsten retains its rigidity at high temperature, allowing extended operation at over 90% of its melting temperature without undue sag or distortion.

In conventional incandescent bulbs, the light comes from the glowing filament and gas is introduced solely to reduce the rate of evaporation of W atoms from the filament and thereby increase the life of the lamp. The presence of the fill gas also reduces the efficiency of the lamp by cooling the filament. With a straight wire, the cooling effect would dominate, but for coiled filaments, the heat loss is reduced significantly and the combined effect is beneficial. Most household lamps are filled with Ar gas at around 600 Torr at room temperature, producing a pressure close to one atmosphere in operation. Another positive effect of the fill gas is to moderate the increase in temperature of the glass envelope, permitting the use of inexpensive soft (lime) glass. Typically, deposition of tungsten atoms on the glass reduces the transmittance by about 10%.

Halogen Lamps

The performance of incandescent lamps can be be improved by increasing the fill pressure, which increases the possibility of explosive failure, or using the heavier, but more expensive, krypton or xenon. The chance of explosions and the extra cost of heavier gases can be ameliorated through the use of more compact bulbs made from glasses, such as fused silica or quartz, that sustain higher temperatures.

With compact lamps, deposition of W atoms on the glass wall causes major problems. Not only does this reduce the amount of light escaping from the bulb, but the resulting heating of the glass envelope can lead to softening and failure, even for

quartz. The solution is to add a component to the gas fill to remove the W atoms from the glass. This can be achieved using halogen atoms, which react with the W atoms to form tungsten halide molecules. At normal operating temperature, the tungsten halide vapor pressure at the wall is above the condensation point, so that the build-up of tungsten on the wall is avoided. In the hotter regions near the filament, the tungsten halide molecules dissociate, and many of the W atoms return to the filament, whereas the halogen atoms are free to diffuse back to the walls.

The active ingredient in early tungsten halogen lamps was iodine. However lamp manufacture is then more difficult, since iodine is a solid at room temperature and oxygen needs to be added to produce a stable tungsten-halogen cycle. Further, iodine absorbs blue light and reduces the perceived color temperature of the lamp. The element preferred in current halogen lamps is Br, which can be introduced in several forms, such as HBr, CH_3Br or CCH_2Br_2. Both fluorine and chlorine have been found to be too corrosive for use in commercial products.

The efficiency of both incandescent and tungsten-halogen lamps can be increased through the use of filters which reflect infrared light but transmit visible light. These often are constructed as multilayers, for example with a mixture of Ta_2O_5 and TiO_2 for the high refractive index material and SiO_2 for the low index layers.

Fluorescent Lamps

The introduction of active plasmas into lamp technology around 1940 led to a three-fold increase in efficiency. The first key advance was the use of mercury vapor as a source of radiation. Some of the positive characteristics of Hg as an emitter are the wide spacing and low excitation energy of the key radiative levels and the presence of neighboring metastable states, which feed excitation into the desired levels. The hyperfine line structure of natural mercury reduces the imprisonment of the radiation, and it is relatively easy to maintain Hg vapor at mTorr pressures. The fact that the primary radiation from mercury is in the UV at 254 nm is not a major disadvantage, since efficient, stable phosphors exist to convert this radiation into visible light.

The major disadvantage of the use of mercury is the environmental impact. Although relatively small amounts are used in each lamp and the low vapor pressure at room temperature reduces the risk of air-borne dispersion, the very large numbers of lights in use and the high toxicity of mercury causes concern.

In fluorescent lamps, the radiating vapor atoms are excited by electron impact, either directly from the ground state or indirectly through metastable or ionic states. Over 80% of the applied electrical power is delivered to the positive column of the discharge rather than to the sheaths, where the energy is mostly lost to electrode heating. Over two thirds of this fraction is converted to UV radiation and the efficiency of the phosphors in converting to visible light is around 40%. Allowing for a small amount of direct visible light from the Hg atoms, the efficiency of transfer from electrical power to

visible radiant power is close to 30%. The spectrum can be tuned to give around 350 lumens per radiant Watt.

In low pressure sodium lamps, the efficiency with which energy is transferred to visible light is also around 30%, but the higher response of the eye to yellow light results in greater overall efficiency. However, the color spectrum is not acceptable for most applications.

The partial pressure of mercury in fluorescent lamps is typically around 5-10 mTorr. The remainder of the 1-10 Torr is made up with a rare gas. Krypton provides highest efficiency for low power lamps, argon is better at intermediate power levels and neon is best at high power.

The major limitation of traditional fluorescent lights is their size and shape, which is necessary to provide an effective positive column at low pressures.. In recent years, considerable effort has been expended in the design of more compact lamps suitable as replacements for less efficient incandescent bulbs. Another innovation has been the use of electrodeless RF discharges for longer lifetimes.

Analysis of the data needs for the low pressure discharge lamps outlined above is given in the accompanying article by Sommerer.

Electrodeless Lamps

In discharges with electrodes, the strongest fields are found in the cathode fall region. In glow discharges, potential drops of the order of 100V are needed to ensure sufficient flow of positive ions to the cathode to maintain the discharge through secondary emission. In arc plasmas the potential drop is smaller, but the ion flux must be able to heat the cathodes to temperatures at which field-enhanced thermal emission of electrons occurs. Acceleration of ions across the cathode fall and consequent electrode heating leads both to energy loss from the discharge and to cathode erosion through sputtering and enhanced evaporation. Loss of material from the electrodes not only limits the lifetime of the lamp, but also the deposition of the cathode material on the glass envelope reduces its transparency. Operating lifetimes in excess of 50,000 hours can be obtained in lamps without electrodes, allowing street lights to function for around 15 years without replacement.

Electrodeless discharges were discovered over 100 years ago (see e.g. Hittorf (2) and Thomson (3)) and crude lamps were constructed by Tesla (4). These discharges have been used for many years in spectroscopy, but study of their properties has been intensified in recent years because of their suitability for plasma processing. When driven by induction coils in the Radio-Frequency (RF) regime, there are several modes of operation. In the absence of external magnetic field, the "E-mode" is observed at relatively low power levels and is dominated by radial or axial electric fields. At higher power levels, the "H-mode" takes over, in which azimuthal electric fields and magnetic fields are more important. The system acts like a transformer, with the induction coil acting as the primary and the circulating plasma current as the secondary. At the higher

drive frequencies of the microwave regime, these two modes merge. Microwave discharges can be excited either using standing or traveling waves.

One of the advantages of electrodeless lamps is that they can be turned on and off quickly. The absence of electrodes in the lamp also allows one to use more corrosive gases, such as fluorine or chlorine, giving one greater flexibility in tuning the gas mix to give higher efficiency or better color balance. The length and shape restrictions of traditional fluorescent lamps can be overcome and many forms of compact discharges have been demonstrated. The major remaining challenges (5) appear to be in the design of electronic controls that are compact, inexpensive and do not create unacceptable electromagnetic radiation (EMI). The space and EMI problems can be solved more easily if the discharge and electronic controls are in separate units. The popularity of microwave ovens has led to significant price reductions in microwave generators, but still most consumers are prepared to pay more for an oven than for a lamp.

There are niche applications, such as the curing of inks or glues, for which electrodeless lamps are well established, and efficient lamps with long lifetimes for household and office lighting are now available as replacements for incandescent bulbs.

High Pressure Arc Lamps

Fluorescent lamps use non-thermal low-pressure plasmas in which electrons are accelerated to energies much higher than that of the neutral atoms or molecules. Although ions do not pick up much energy in the positive column, they are accelerated across the sheaths and contribute significantly to electrode erosion. The velocity with which ions strike the electrodes can be reduced through the use of higher pressures. In arc lamps, the neutral gas is also heated. The high temperature leads to reduced neutral densities in the arc channel, thus facilitating electron transport. The pressure in these arc lamps range from 1 to 100 atmospheres and peak temperatures are between 4,000K and 10,000K. The envelopes must be more rugged and are often made from fused quartz, polycrystalline alumina or translucent ceramics. These lamps, often called High Intensity Discharge (HID) lamps, and offer high brightness, high efficiency and long operating life, typically 10,000 to 30,000 hours.

The simplest HID lamp uses mercury vapor and tungsten electrodes and is contained by a fused quartz arc tube, with Mo foil seals to allow current to pass through the quartz envelope to the electrodes. The central temperature is around 6000K, whereas the temperature of the quartz tube does not exceed 1000K, since thermal diffusion is moderated by the pressure of several atmospheres. Despite the significant temperature gradients, the discharge is close to Local Thermal Equilibrium (LTE). Typically about 15% of the input electrical energy is converted to visible light.

The efficiency of high pressure Hg lamps can be improved through the addition of sodium, with xenon added as a buffer gas to facilitate ignition. The color dominance of the Na resonance lines is reduced by self-absorption and the presence of Hg and Xe

leads to intense excimer emission in the red. By appropriate selection of gas mixture, pressure and surface materials, high pressure sodium lamps can be tuned to give luminous efficiency over 150 lpw, color balance similar to that of incandescent lights, or lifetimes in excess of 20,000 hours. Unfortunately, simultaneous achievement of these characteristics has not yet been achieved.

High pressure Hg lamps are often modified through the addition of metal halide salts, such as NaI and ScI_3. Although most of the salts remain as a condensate on the arc tube wall, the wall temperature is sufficiently high to support a partial vapor pressure of order of 0.01 atmosphere. Because the excitation and ionization energies of Na and Sc are much lower than those of the denser Hg atoms, the minor components can dominate both the discharge formation and the radiation at the center of the metal-halide discharge. This can lead to a doubling of the fraction of energy transferred to visible light. The dominance of Hg atoms in the outer, cooler regions is important in setting the arc impedance and the thermal conductivity of the discharge.

Iodine is the most common halogen in metal halide (MH) lamps, although bromine and chlorine have also been used. A combination of metals is usually included to provide the desired color balance. Na and Tl are commonly used to provide emission in the red and green portions of the spectrum, while the blue can be supplied by In, Sc, Dy, Ho or Tm.

The chemistry and transport in HID lamps are extremely complex and fully warrant the special attention that is provided by Adler in the accompanying paper. Earlier reviews were provided by Work (6) and by Dakin et al. (7).

Mercury-Free Arc Lamps

The use of mercury in light sources has led to considerable concern about its environmental impact, and there has been growing interest in the development of mercury-free lamps. However, in analyzing the health impact of alternative lamps, one must also consider the indirect effects of changes in efficiency. Burning fossil fuel in power plants releases Hg to the atmosphere in a form that is more dangerous to life than the Hg in lamps that are discarded in land fills. So, for example, the substitution of incandescent lamps for Hg-containing fluorescent lights leads to an increase in the absorption of Hg by biological systems, as well as to additional emission of global warming gases.

A prerequisite of mercury-free lights is therefore that they are at least as efficient as the lamps they replace. One possible substitute is sulfur, but low pressure S lamps are inefficient and high-pressure S lights produce a yellow-green color. Xenon discharges can be designed to be efficient producers of UV light at 148nm or 172 nm, but most of the energy will then be lost in conversion to visible light, unless one can find phosphors which give more than one visible photon for each UV photon absorbed. Another candidate is barium, which can be vaporized at modest temperatures and emits directly in the visible. Unfortunately, the primary emission is a single line in the green, with a

little emission in the red and hardly any in the blue. Nevertheless, investigation of the efficiency of light production in barium discharges is underway.

The growth of the flat panel display industry has provided further incentive for the development of mercury free lamps. Multi-colored images are often produced by the use of filters that separate out the red, green and blue components of the light. Strong emission lines that fall near the borders of these three ranges are either lost or cause difficulties in color control. Both mercury and sodium lamps often have strong yellow components that can be troublesome in this respect. Lamps with just three strong lines, one near the center of each portion of the spectrum, could increase the efficiency of the color modulation system. If the three lines come from different elements, the amount of each component can be tailored to achieve a wide range of color temperature.

The alkaline earth elements, barium, calcium, magnesium and strontium have relatively simple outer shell structure and possess suitable strong lines in the green (Ba) and blue (Ca, Mg and Sr). However, these elements do not function well in arc lamps. Shaffner (8) has suggested the use of indium for blue, thallium for green, and lithium for red, but the practicality of this recipe has yet to be tested. Obtaining a strong source of blue light for flat panel displays seems to be the most difficult challenge, in metal-halide lamps as well in light emitting diodes and electroluminescent sources.

Dielectric Barrier Discharge Lamps

Dielectric barrier discharges (9) are created by covering metallic electrodes with a thin layer of insulating material. When driven by AC circuits over a wide range of frequencies, these discharges consist of a series of many narrow streamers with radii of order 100μm and lifetimes of a few ns. Non-thermal plasmas can thus be produced even at pressures above 1 atmosphere and electrons with energy of 1-10 eV can be generated efficiently. Electron densities of over 10^{14} cm^{-3} are achieved, giving currents of about 0.1A in each micro-discharge. Conversion efficiencies of up to 60% have been reported in the conversion of energy deposited into Xe discharges into UV light at 148 nm and 172 nm. There are as yet no phosphors to convert this UV radiation to visible light with high efficiency, but these discharges provide excellent sources of UV light for material modification (10) or pollution control applications (11).

Shorter wavelengths can be obtained by using pure Ar (126 nm) or Kr (146 nm) excimers, and longer wavelengths can be produced efficiently by mixing F or Cl with the rare gas.

ELECTRONIC DISPLAYS

For the past sixty years the electronic display industry has been dominated by cathode ray tubes. Technological progress has been steady, but relatively slow; the major concern is to minimize costs as the performance levels increase. The

technological challenges relate to electron beam formation and transport, phosphor efficiency and stability, and general electronics issues. Access to improved atomic and molecular data is not a high priority in this segment of the industry.

The search for alternative technologies has been driven by a desire to reduce the size and weight of the display, while improving the quality of the image. Although laboratory studies have been underway for many years, the availability and performance of commercial products were very limited until the 1980's, when Japanese companies courageously began to invest billions of dollars in the development and fabrication of liquid crystal displays, first as viewfinders in cameras and camcorders and then in portable computers. This foresight led to almost complete domination of the FPD industry, with over 95% of the production coming from Japan. This dominance is now being challenged, primarily by Korean and Taiwanese companies, but the manufacturing experience, industry infrastructure and broad patent portfolios of the pioneering companies give them great advantages in maintaining business leadership.

Liquid Crystal Displays

The major scientific bases underlying liquid crystal displays (LCD) are in condensed matter and optical physics. For conventional LCDs the impact of atomic and molecular data is mainly in the design of the light source. In the large area displays used for notebook computers, compact fluorescent tubes are used as backlights or on the edge of the screen, with deflector systems to direct the light through the pixels. Both hot and cold cathodes are used in these miniature tubes. The cold cathodes require higher starting voltage and are less efficient, but they reduce problems from overheating and give longer lifetimes.

Small liquid crystal panels are now being used to create the images within projection systems. The demands for long lifetime and high efficiency leads to the use of high pressure lamps with very small arc gaps, filled with mercury, metal-halide mixtures or xenon. There is currently a particular need for the development of efficient lamps with lifetimes in excess of 10,000 hours that can be focused onto light modulators of diagonal size less than 1".

Since the transmission efficiency of liquid crystal modulation systems is low, usually 3-5%, much current research is aimed at the development of reflective light valves, which make use of ambient light, or emissive displays, which provide their own light. Emissive displays are discussed below.

The transmission of polarized light through liquid crystal cells depends on their orientation, which can be modified through the application of electric fields. In passive matrix devices, the potential difference across each pixel is controlled directly from the voltage applied to the relevant row and column drivers. However, this simple approach provides limited contrast and response speed, which can be improved by the introduction of non-linear elements. In active matrix LCDs this is usually achieved by fabricating thin-film transistors at each pixel. Although millions of TFTs can now be

made on a single panel, the yield of good panels falls rapidly with increasing substrate size. Gas discharge physics provides an intriguing alternative.

Plasma Addressed Liquid Crystal Displays

In active matrix LCDs, each pixel is controlled by a separate thin film transistor (TFT). In PALC displays (12), the thousands of TFTs in each row are replaced by a single plasma channel. The role of these channels is not to create light, but solely to act as a switch. This replacement avoids many of the complications of AMLCD manufacture and provides a simple way to build large area LCD panels.

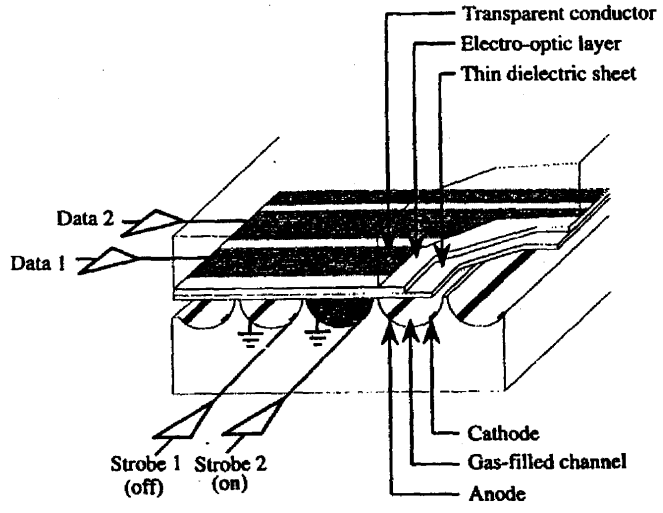

FIGURE 2. Structure of the Plasma-Addressed Liquid Crystal Panel (Courtesy: K. J. Ilcisin)

As shown in Figure 2, the liquid crystal material is contained by the color plate on one side, with embedded column electrodes, and a dielectric microsheet on the other. The plasma channels are formed between this microsheet and the second glass substrate, with barrier ribs separating the rows. Parallel cathode and anode electrodes are formed along each channel, either on the surface of the second substrate or on the barrier ribs. When a voltage of about 350 volts is applied between the anode and cathode, a plasma is formed, creating a virtual electrode on the surface of the dielectric layer at a potential close to that of the anode. The data voltage of about 70V applied between this virtual electrode and a column electrode is sufficient to align the liquid crystal molecules.

The two major concerns in the selection of gases are the panel lifetime and the switching speed. Since the electrodes are exposed to the plasma, the use of highly reactive gases would reduce the lifetime. The first choice is thus one of the rare gases, or perhaps a mixture, and VGA panels have been constructed using both He and Xe.

Gas breakdown is relatively rapid and so the switching speed is determined primarily by the rate of decay. In single-component rare gases, this decay is slowed significantly by the formation of metastable states. Nevertheless, the 30μs cycle times required for VGA panels can be achieved. For high-resolution monitors or HDTV, cycle times of 15μs are required. One way to quench the metastables is through a Penning mix, but this may just lead to the replacement of one metastable by another. Another solution is to add a molecule that can dissociate to absorb the extra energy. Ilcisin et al (13) have shown that decay times less than 5ms can be achieved with a He-H_2 mix, allowing the addressing of 3000 lines within a 60 Hz frame rate. The use of H_2 provides challenges in attaining a long lifetime, but the preliminary results are extremely encouraging.

Emissive Displays

Multicolor flat panel displays use solid-state phosphors to create the light. In electroluminescent (EL) and field-emission displays (FED), the phosphors are excited by electron impact. Field emission devices are leading to a renaissance in the art of vacuum tube technology, but require little new atomic or molecular data. In some senses, they are like cathode ray tubes in that electrons are accelerated at low pressures onto a phosphor screen. In CRTs the electrons are drawn from a single cathode and directed onto the appropriate spot on the screen by electric and magnetic fields. The distance between cathode and screen must be of the same order as the screen diagonal and large screen CRTs are necessarily bulky. In FEDs, the gap is very small and each pixel has its own source of electrons. Cold cathodes are used, made from low work function materials often shaped into narrow cones to enhance the electric field strength near the surface.

EL displays and light emitting diodes (LED) employ solid state technology and are even further removed from atomic and molecular physics. This leaves only one emissive FPD technology, the plasma display, for our attention.

Plasma Displays

The early plasma display panels produced monochromatic light and were essentially arrays of neon lamps. Today's color PDPs (13) are more analogous to fluorescent tubes, in that the gas discharge produces UV radiation which is converted to visible light by phosphors. Since the vapor pressure of mercury is too low at room temperature, xenon is used as the active gas.

Plasma panels are better suited to larger displays, indeed it is very difficult to manufacture plasma displays with pixel sizes less than 100 microns. Diagonal sizes around 40" are now standard for TV applications. Semiconductor manufacturing techniques are much less important than in other types of display.

Panel Architecture and Operation

Most plasma displays consist of an array of parallel discharge channels of height and width around 200μ, separated by barrier ribs, between two glass substrates. The channel surfaces are coated, on three sides if possible, by phosphor material, with red, green and blue phosphors in separate channels. The fourth side is transparent to let out the light. The channels are filled with rare gas mixtures at a pressure of about 400 torr. The active xenon gas is usually a minor constituent in a buffer gas of helium, neon or a He-Ne mixture.

Plasma displays are driven by applying high frequency voltages, either in AC or DC mode. In the more common AC devices, the electrodes are embedded in a dielectric film, so that current flow leads to the formation of a wall charge. Each half-cycle, the charge that was deposited on the dielectric during the previous half-cycle magnifies the applied field and contributes to discharge growth. This reduces the voltage needed to sustain the light production and provides a memory effect. If the voltage of the sustain pulse is just insufficient to cause breakdown, light is created only in those pixels with wall charge. The dielectric film is protected with a thin layer of MgO, which has a high coefficient of secondary electron emission to maintain the discharge during each pulse. Despite many searches, a better emitter of secondary electrons than MgO has not yet been found

In AC panels, at least three different pulse shapes are needed, one to turn individual pixels on, by creating a wall charge, another to turn pixels off, and the third to sustain the discharges in all pixels that are "on". The addressing of individual pixels is accomplished by orienting the electrodes on the two substrates in perpendicular directions.

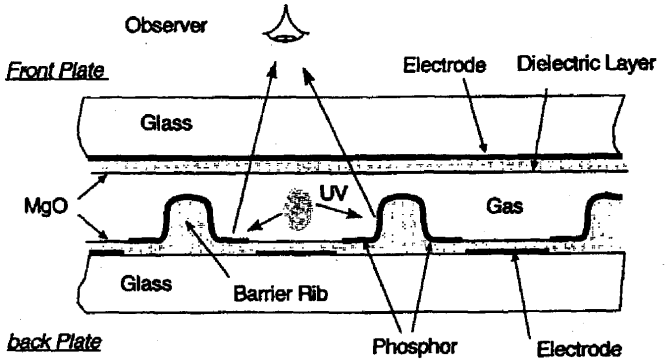

FIGURE 3. Opposed electrode structure of a plasma display panel. (Courtesy: J. P. Bouef).

There are two forms of AC display. The simpler structure, shown in Figure 3, has two sets of electrodes, one on each substrate, that are used both to supply current and to switch the discharge on and off. This form is referred to as the dual-substrate,

opposed electrode or matrix structure. The electrodes run in perpendicular directions, with those on the lower electrode running down the channels defined by the barrier ribs. The presence of these electrodes reduces the amount of surface area that can be covered with phosphors.

The second structure, as shown in Figure 4, has dual (parallel) electrodes on the upper substrate that create a surface discharge between each pair. This form has been called the single-substrate, surface discharge or coplanar structure. The barrier ribs are again built upon the lower substrate, running in a direction perpendicular to that of these electrode pairs, to define the discharge channels. A single electrode runs along each channel on the lower surface and is used solely for addressing. The addressing electrodes are covered with a dielectric layer, but are not subjected to bombardment by energetic ions and so can be covered with phosphor material rather than MgO.

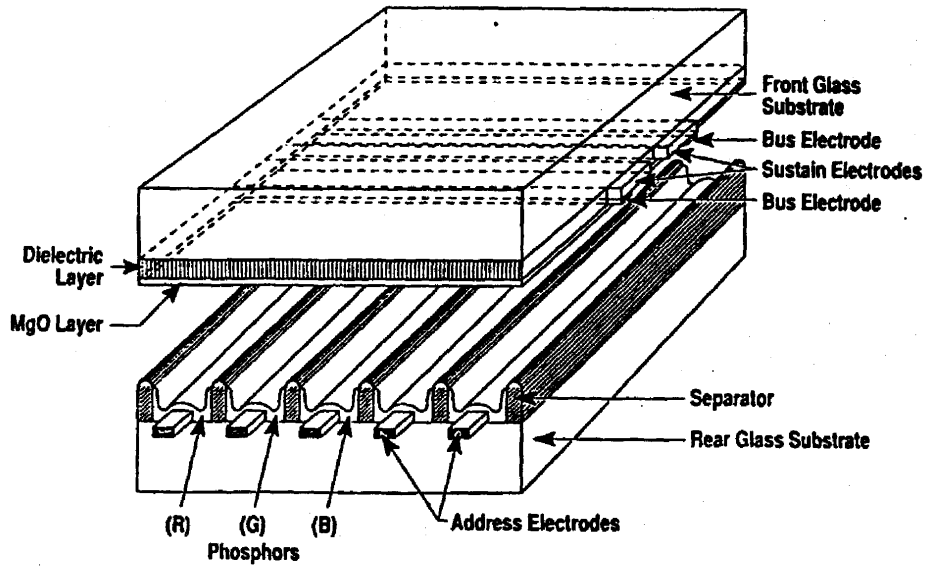

FIGURE 4. Structure of the surface -discharge plasma display panel. (Courtesy: Fujitsu)

The dielectric layer in AC displays also limits the current growth during each half-cycle. In DC discharges, the electrodes are in direct electrical contact with the plasma and a capacitor must be added to prevent runaway. Memory is usually achieved through auxiliary discharges which act as triggers for subsequent pulses. In some DC devices, barriers are constructed in both directions, so that each pixel is separated from its neighbors, to reduce "cross talk".

Gas Discharge Physics

The major challenges in discharge physics are to choose the gas mix, wall materials, pixel geometry and electrical pulse shapes for optimal performance.

The efficiency of transfer of electrical energy to emitted visible light is typically around 1%, which is almost two orders of magnitude less than that of a fluorescent light and leads to a relatively high power consumption for plasma displays. Problems arising from variations in the breakdown voltages at different points along each channel, and over time as the display ages, can be reduced by increasing the "voltage margin", that is the difference between the minimum and maximum voltages that will sustain the light in "on" pixels without causing breakdown in "off" pixels. Panel lifetime is another major concern; sputter damage to phosphors and MgO should be minimized and the gas mixture should remain constant. Operating lifetimes of 30,000 hours are now claimed.

Color control is obtained not by changing the intensity of the light but by varying the length of time that each pixel is on. Up to 256 brightness levels for each color have been obtained, but more would be desirable for the elimination of artifacts in portraying moving objects. This would be facilitated by faster discharge formation and decay.

Experimental development of PDP discharges has been retarded by the lack of detailed diagnostic data. Computer simulations have been developed in recent years by several groups. 1-D simulations can be carried out using fluid, kinetic and hybrid methods, but the kinetic methods are very time consuming in 2-D or 3-D. 2-D fluid models (15-17) are valuable, but it is important to understand the limitations of these models and to develop hybrid techniques (18) where necessary.

Most of the relevant atomic physics is already present in 1-D models. Veerasingham et al (19) have recently published a 1-D fluid model for a He-Xe panel including 3 states of neutral He, 7 states of neutral Xe, the ground states of He^+ and Xe^+, and Xe_2 excimers. No molecular ions are considered. Collisions of excited atoms are very important, both with electrons and in Penning ionization and dimer formation. Collisional broadening controls the radiative line width and therefore the extent of trapping of the atomic UV radiation.

Veerasingham et al (19) suggest two possible reasons for the low efficiency of plasma displays in comparison with fluorescent lamps. The first is the small size. The efficiency of miniature fluorescent lamps is also less than that of the larger versions, but progress is being made through their use as backlights for LCDs. The second factor is the need for rapid switching of PDP discharges. Both of these factors mean that the more of the discharge energy is deposited in the cathode fall region, rather than in the positive glow region. Perhaps a more useful comparison could be obtained with dielectric barrier excimer lamps, which attain high efficiency of UV production with relatively small electrode gaps and short-lived microdischarges. However, Falkenstein and Coogan (20) have shown that the efficiency of UV production from XeBr in dielectric barrier discharges decreases from 7% to 4% when the gap size is reduced form 5.5 mm to 2,5 mm. This is still well above the 200 μm gap typical of plasma displays. A third factor reducing the overall efficiency comes from the greater energy loss in conversion from UV to visible light using single-photon phosphors.

The leading commercial producers of PDPs currently use Ne-Xe mixtures, for which models have been developed by the Toulouse group (15,21,22). These models do

include molecular ions, but their densities are small compared to that of Xe^+. For the particular parameter set assumed in reference (15), the models confirm that over half of the energy deposited into the plasma goes into ion acceleration, with only about 15% going into xenon excitation.

Discharge Diagnostics

To address issues concerned with display uniformity and the interactions between neighboring pixels, electrical and optical data on individual pixels is valuable. Measurements of the UV output are particularly challenging, since the materials used in PDP construction absorb the UV radiation. Special diagnostic panels must therefore be built, using transparent materials, such as MgF or allowing for observation along the channel. Unfortunately, this latter approach does not provide information on individual pixels. Pioneering work in this field has been performed by Tachibana et al (23), but much more study is needed.

SEMICONDUCTOR MANUFACTURING

Plasma processing involves the use of ionized gases in the production of solid or liquid materials with special properties. Since low temperature plasmas interact only with the surface of the condensed matter, they are most useful in the formation of thin films and so are particularly valuable in the semiconductor manufacturing industries. Almost all of the scientific effort in the U. S. concerned with plasma processing is focused upon semiconductor applications. The effort is more broadly based in the rest of the world, but the global economic impact is also dominated by the application to the microelectronics industry. An excellent introduction to the basic physics involved in plasma processing can be found in the book by Lieberman and Lichtenberg (24).

Plasma processing can be divided into three categories, depending on whether the goal is to add, remove or modify surface material. Once again, this article is not designed to be completely comprehensive; it is focused upon the most important subtractive and additive processes.

In surface modification, the plasma is used to change the chemical composition of the outer layers of the material or to change the physical or chemical properties of the surface. Usually the goal is to improve the resistance of the surface to external damage, whether by chemical attack, abrasion or impact, or to passivate the surface so that it becomes mechanically or chemically inert. For example, plasma nitriding (25, 26) is often used to improve the strength of metal surfaces. Sometimes, however the purpose of the plasma treatment is to make the surface more active. For example, plasma processing can increase the absorption of paint or inks by plastics.

One topic that has received much attention in the research community is plasma-immersed ion implantation (PIII) (27) . Most commercial ion implantation is done with accelerators, creating ions at low pressure and accelerating them onto the work-piece

at energies at energies between 10^4 and 10^7 eV, depending on the desired doping depth. This is well suited to the treatment of planar surfaces. In PIII the work-piece is immersed in a plasma and suddenly given a high negative bias. Ions are then drawn into the surface at high velocity. PIII can be used not only for planar surfaces, but also for small components that need to be implanted from all directions. However, despite many years of intense effort, the adoption of PIII by industry has been slow.

The simplest type of plasma reactor has two parallel electrodes that are driven by an RF potential, usually at 13.56 MHz. Such reactors are often called reactive ion etchers (RIE) and are most efficient at pressures around 100 mTorr. The energy is deposited through capacitive coupling. One major disadvantage of simple diode reactors is that the plasma density and ion energy cannot be varied independently. The addition of magnetic fields, in magnetically enhanced reactive ion etchers (MERIE), provides an extra variable parameter and allows operation at lower pressures, as does the introduction of a third electrode in triode reactors.

Much attention has been given in recent years to low pressure high density reactors, in which the electron density can exceed 10^{12} cm^{-3} at pressures around 1 mTorr. The type used most commonly by U. S. industry is the inductively coupled plasma (ICP) reactor (28, 29, 137-140). The plasma is created through inductive coupling from RF current flowing in a coil which is separated from the plasma by a dielectric window. The substrate holding the work-piece is driven by a second RF circuit and develops a DC bias, which draws the plasma ions onto the wafer. Variation of the relative power levels in the two RF circuits provides separate control over plasma density and ion energy. Inductive reactors seem to scale well in size. The transition in semiconductor processing from 200 mm wafers to 300 mm wafers should cause few problems, since ICP reactors have been used successfully for uniform etching of flat panel display substrates measuring 600 mm by 720 mm.

In electron cyclotron resonance (ECR) reactors (30), the plasma is created by the resonance absorption of microwave radiation, usually at 2.45 GHz, in an external magnetic field. These reactors can be operated at even lower pressures, below 1 mTorr, and are popular in Japan. However, they have not been widely adopted in the U. S., probably due to their extra complexity. ICP plasmas can also be enhanced through the use of magnetic fields. One such device is the helicon (31), in which the electron density is increased by the propagation of very low-frequency waves. Although helicon reactors have led to considerable academic interest, they have achieved only limited commercial success.

Physical Vapor Deposition

Physical vapor deposition, or sputtering, is used to create layers of metals, alloys or insulators in a wide variety of industries, including semiconductor manufacturing. In its simplest form, physical sputtering, a plasma is created to remove atoms from a target by ion impact and transport the neutral atoms over to the work-piece. Argon plasmas

provide efficient sputtering with minimal reactions of the sputtered atoms in transit. Pressures of a few mTorr are used to reduce losses due to elastic collisions. DC glow discharges cannot easily be maintained at such pressures and magnetron discharges are favored. In magnetron reactors, permanent magnetic fields are used to trap electrons and increase the probability of the electron impact ionization that is needed to maintain the discharge. Physical sputtering is used for a broad variety of metals and alloys.

Reactive Sputtering

A greater range of deposition layers can be obtained through the use of reactive sputtering (32-34). Molecular gases are introduced and the plasma parameters optimized so that the chemical reactions lead to the desired stoichiometry in the deposited material. The properties of the layer can often be improved by controlling the temperature of the substrate and the energy and flux of the ions that strike the substrate.

Reactive sputtering is widely used to deposit dielectrics, such as oxides and nitrides, as well as carbides and silicides. Common reactive gases are O_2 and H_2O for O atoms, N_2 and NH_3 for N atoms, CH_4 and C_2H_2 for C atoms and SiH_4 for Si atoms. Reactive sputtering is often necessary even when the deposited and target materials are the same. For example, depositing insulating layers of SiO_2 from an SiO_2 target directly by physical sputtering leads to silicon-rich films. The 1:2 Si/O stoichiometry can be restored by the addition of O_2 to the Ar feed gas. Alternatively, SiO_2 layers can be produced from pure silicon targets, by using gases containing oxygen (33).

Ionized Physical Vapor Deposition

In many deposition tasks, the goal is to deposit a layer of uniform thickness over the whole workpiece. However, the development of semiconductor devices with multiple metal layers and the continued reduction in feature dimensions require the deposition of metals to the bottom of narrow trenches and holes. Since neutral atoms approach the surface from all directions, they will stick on the sides of the feature and prevent access to the bottom. The solution is to create a high-density plasma in which the majority of the sputtered atoms are ionized and accelerated by the substrate bias voltage at right angles to the work-piece. This approach (35,36) is now called ionized physical vapor deposition (I-PVD).

Both plasma and surface processes are important in reactive sputtering, to assure the correct stoichiometry and the required physical properties of the deposited films. Surface reactions on the reactor walls, as well as on the sputter target and workpiece, can affect the balance of ions and radicals in the plasma. Although there have been recent empirical studies of the correlations between film quality and the plasma

parameters, the development of comprehensive models has not received as much attention as for chemical vapor deposition (CVD) and etching.

Chemical Vapor Deposition

The deposition of elements that can be extracted from gaseous compounds was traditionally achieved by chemical vapor deposition. The desired atoms are freed thermally, so that the major adjustable parameters are temperature, pressure and the flow rates of each component in the gas mixture. Ionizing the gas provides much more control over the process, producing more radicals as well as ions and avoiding the need for high substrate temperatures, which may lead to damage. This process is usually called plasma-enhanced chemical vapor deposition (PECVD).

The deposition of hydrogenated amorphous silicon (a-Si:H) plays a very important role in the manufacture of active matrix liquid crystal displays and in photovoltaic devices, such as solar cells. The common approach is to use an SiH_4/H_2 discharge in an RF reactor. 2D models, involving electrical, thermal and chemical modules, have been recently developed for these discharges and have been compared against laser-induced fluorescence measurements of radical densities (37,38).

Three types of ions are included in this model, light positive ions, such as H_2^+, along with the high mass +ve and -ve "mean" ions, SiH_m^+ and SiH_m^-. The electrons are described by three moments, density, momentum and energy, in the standard fluid approximation. However, the chemistry is dominated by the neutral radicals. The source of these radicals is assumed to be electron impact dissociation of the molecules SiH_4, Si_2H_6 and Si_3H_8. The radicals that are followed are H, SiH_n (n-0-3) and Si_2H_n (n=2-5). The Palaiseau group has provided excellent analyses of the collision processes in the plasma (39) and on the substrate (40).

The growth of particulates in plasma reactors for semiconductor manufacturing can be very deleterious and there has been considerable study of the growth and transport of dust particles. Much of this work has been focused upon silane plasmas, but there appears still to be disagreement over the relative roles of SiH_2 radicals, SiH_3 radicals and negative ions in the nucleation and growth of particulates (41-43).

Silane mixtures are also used in the production of dielectric materials by PECVD. For silicon nitride (Si_3N_4), the added gas may be N_2 (44,45) or NH_3 (45,46), whereas NO_2 can be added to give the oxynitrides SiN_xO_y. The most commonly used dielectric, SiO_2, can be produced from mixtures of SiH_4 with an oxygen donor such as O_2 (47), NO, N_2O or H_2O_2, usually diluted in Ar (48). A typical chemistry model for SiO_2 deposition can be found in the paper by Meeks et al. (47). Since silane is explosive at room temperature, a popular alternative Si source is tetraethoxysilane ($Si(O\ CH_2\ CH_3)_4$ or TEOS), which is a relatively inert liquid (49). A fascinating study of the ions and neutral fragments produced in a TEOS/Ar discharge has recently been presented by Basner et al (50).

The need to reduce the wiring capacitance in integrated circuits as metal spacimgs are reduced to below 0.5 micron has led to the search for intermetal dielectric films with lower dielectric constant (k) than that of SiO_2, which is 3.9. One possibility is to use organic polymers. Another approach is to dope SiO_2 with boron nitride, boron oxide or fluorine. Fluorinated SiO_2 films can be deposited by PECVD by modification of the gas mix. Han and Aydil (51) have produced films with k = 3.2 using a simple SF_4/O_2 mix, whereas Yoshimaru et al (52) use a more complex gas containing TEOS, He, O_2 and C_2F_6.

Dry Etching

The need for dry (plasma) etching, rather than wet (chemical) etching, has increased as the dimensions of semiconductors have shrunk. The creation of narrow trenches or holes with vertical sidewalls demands anisotropic etching, and the need to cut through one layer without damage to very thin underlying layers of different materials requires excellent selectivity in the etching process. Etching rates inside holes or trenches depend on the aspect ratio of the feature as well as on the density of nearby features that are being etched simultaneously. The gas mix is chosen to minimize these effects and to maintain control over feature shape, avoiding notches and protrusions. Plasma processing is ideal for etching in that the directionality of the incident ions provides a capability to fabricate vertical walls. Plasmas can also be turned off rapidly compared with etching times scale (tens of seconds) so that when one layer is completely etched, the process can be stopped with minimal damage to the underlying layer. A change in the material being etched often leads to changes in the plasma behavior that can be detected, either from the optical emission or the response to applied RF fields. This provides a signal that can be used to terminate etching.

In semiconductor equipment manufacturing companies, etch processes are often sub-divided into three categories, silicon, metal and dielectric.

Silicon Etching

Although the etching of amorphous silicon is important in the AMLCD and photo-voltaic industries, the demands for narrow feature size are not so demanding and so most attention has been paid to the etching of polysilicon and silicides for the IC industry. As an example of the challenges that will soon be faced, Tennant et al. (53) envisage a transistor with a 70 nm channel length. At its heart is a gate stack with 80 nm of tungsten silicide (WSi_x) on top of 100 nm of polycrystalline silicon. Underneath the stack is dielectric layer of SiO_2 of less than 2 nm in thickness. Etching through the stack and removing all the unwanted polysilicon, without breaking through the dielectric, remains the benchmark task.

Although fluorine etches Si rapidly, it is in fact too aggressive, since the etching is isotropic and the selectivity is poor. Chlorine and HBr are most commonly used as the

active etchants, with possible admixtures of Ar and O_2. There is always interest in looking for alternative etchants, such as HI (54) and NF_3.

Great progress has been made in recent years in the analysis of the etching of polysilicon in chlorine plasmas. Etching proceeds through the formation of chlorinated surface layers, through the absorption of Cl, Cl_2 , Cl^+ or Cl_2^+, followed by ion-induced sputtering of $SiCl_x$ molecules. Although both Cl atom and Cl_2 molecules stick readily to pristine Si surfaces, as the Cl coverage increases, the absorption of Cl_2 molecules drops and the presence of Cl atoms is essential to maintain a high etch rate. Fourier-transform infrared (FTIR) absorption measurements (55) show that the major reaction product leaving the surface is $SiCl_4$, although other SiClx molecules are observed in the surface layers.

The etch rate depends not only on the energy and flux of neutrals and ions striking the surface, but also upon the flux of reaction products returning to the surface and of molecular fragments from resist erosion. Recent experiments by Choe et al (56) have shown that the levels of ionization and dissociation are both sensitive to the condition of the reactor walls and change slowly as more etching is accomplished. This is attributed to reduction of the rate of chlorine atom association on the walls due to the deposition of etching products. Molecular dynamics simulations of chlorine atom association on several of the surfaces found on wafers and reactor walls have been reported by Kota et al (57). More experimental checks of these calculations would be valuable.

This progress has been achieved through the work of many groups, using a wide variety of techniques. Beam studies of the etching reactions (58-62) have shown how the etch rate varies with the variation of single parameters, such as the energy or angle of approach of the incident ions or the degree of pre-absorption of chlorine into the surface layers. However, great care must be taken in the application of such data to etching in a real discharge, since there are many variable parameters. There appears to be an effective threshold around 20 eV for rapid ion-induced etching of Si by Cl. The corresponding threshold for SiO_2 removal is over 50 eV, and high selectivity can be obtained by arranging the impact energy of the incident ions to lie mainly between the two thresholds. The chemical state of the surface during etching has been studied by in-situ infra-red spectroscopy (55), by laser-induced fluorescence studies of laser desorbed molecules (56) and by X-ray photoelectron spectroscopy (63). Optical emission actinometry (64),two-photon laser-induced fluorescence (65) and mass spectrometry (141,142) have been used to measure the degree of dissociation of the chlorine plasma. Plasma models (66-68) have been extended to include surface reaction chains as well as collision processes within the discharge. The models attempt to predict the evolution of feature profiles as well as average etch rates and so provide more opportunities for checks against experiment.

Many forms of silicon are used in the semiconductor industry. In addition to variations in the crystal structure, silicon is often doped with electron donors or acceptors. Usually the etching chemistry must be adapted for each particular variety. Sometimes one wishes to etch continuously through two or more silicon layers in a

single step and thus must make a compromise in the choice of chemistry, but the greatest challenge is to be able to etch one variety of silicon selectively with respect to another.

Metal Etch

The metal that is most commonly used in semiconductor chips is aluminum, often in alloy form with small amounts of another metal, such as copper or neodymium, added to reduce electromigration and prevent the formation of surface hillocks during deposition. The aluminum may be sandwiched between metallic thin films, such as TiN, to improve electrical contact. Aluminum can be etched anisotropically using chlorine based gas mixtures. When Al is exposed to air, a layer of aluminum oxide is formed rapidly. This layer is usually called native oxide. BCl_3 is usually added to the etching gas to break through this oxide layer. Other gases, such as Ar, O_2, or N_2 are often added to optimize the process. For example, the addition of O_2 can lessen the dependence of the etch rate on aspect ratio as well as increasing the rate (69).

Kazumi et al (70) have recently published a valuable analysis of the dissociation and ionization pathways in BCl_3 plasmas and the relationship between the plasma chemistry and etching parameters in BCl_3/Cl_2 mixtures, including a discussion of the etching of TiN and resist material. Another comprehensive plasma chemistry model has been developed by Meeks et al. (71). The effects of the negative ions in such plasmas have been studied carefully by the Sandia (Albuquerque) group (72,73).

Although the degree for selectivity required in etching metals and dielectrics is not as high as for polysilicon, minimization of the etching of the walls of narrow features is critical. It has been suggested that deposition of photoresist fragments on the walls reduces the etching (74), which could explain the observed dependence on the ratio of resist to metal.

There has been much discussion about the replacement of aluminum by copper. Although its higher conductivity makes it attractive, the difficulty of etching copper has delayed its introduction for several years. An alternative is to deposit the metal into pre-existing channels and remove the excess by chemical-mechanical polishing (CMP).

Dielectric Etch

The controlled, anisotropic etching of dielectrics such as SiO_2 selectively with respect to Si is a formidable challenge. High ion energies are required for rapid etching and energetic ion often sputter indiscriminately. The key is to deposit protective polymer films on surfaces that should not be etched, such as the walls of dielectric trenches and the underlying silicon layers. This is achieved through the use of fluorocarbon gases, the simplest of which is CF_4.

The feedstock gas must provide an appropriate mix of F atoms to do the etching and radicals to build the fluorocarbon polymer layer. The simple CF_4 gas usually provides too many F atoms. The balance can be improved by using a compound with a greater

C:F ratio (75), such as C_2F_4, C_2F_6, C_3F_6, C_3F_8 or C_4F_8, or by introducing hydrogen, which extracts F atoms to form HF. The latter can be achieved by adding H_2 (76), CH_4 (77), or through the use of incompletely fluorinated methane constituents, CH_xF_y (78). Although hydrogen is very effective at abstracting F atoms from the discharge and the polymer layers, Bjorkman et al (79) have suggested that its presence will cause problems in the etching of features with very high aspect ratios.

Although polymer deposition enables selective etching of dielectrics with respect to polysilicon, the simultaneous deposition and etching adds considerable complications to models of profile evolution in oxide and nitride etching. The polymer films may also be deposited on the reactor walls. Since the plasma chemistry is sensitive to the condition of the walls, significant changes can occur through continued use of the reactor. The etching parameters drift with time and wall cleaning is a major concern in the design of etching systems for dielectrics.

Standaert et al (80) have shown that during etching by such mixtures, the protective fluorocarbon layers on polysilicon surfaces are typically 2-7 nm thick and conclude that the Si etch rate is determined by the rate of F atom diffusion through the layers. They suggest that the incorporation of H into the fluorocarbon layer slows this diffusion through the formation of HF molecules and thus suppresses Si etching even further.

The mechanism by which the protective layers are built up is as yet uncertain. Stoffels et al (81) have used electron attachment mass spectrometry to study polymer formation within the discharge. They find fully saturated polymers $F(C_nF_{2n+2})$ in CF_4 plasmas. As the amount of fluorine in the parent gas decreases, the polymers become less saturated. They are then more reactive and may more easily attach to receptive surfaces. This work supports the thesis that the polymers are formed in the discharge and then transferred to the silicon. Others suggest that it is small radicals that stick. Inayoshi et al. (82) have injected the long-lived CF_2 radicals into Ar and H_2/Ar plasmas and studied their adsorption on Si surfaces. They find that the presence of the plasma enhances the sticking rate, more in the case of Ar than in the H_2/Ar mix. The effect is so large that they believe that the ion bombardment from the plasma makes the surface more receptive to CF_2, but that H adsorption passivates the surface layer. They do not discuss the possibility that the plasma is dissociating the CF_2 to form more reactive radicals, F and CF. Clearly more studies of this kind are needed.

The interaction of fluorocarbon and hydrocarbon ions and radicals with reactor walls also deserves attention. Sugai et al (83) have studied collisions of CF_4^+ and CH_4^+ ions on aluminum. As soon as the ion beams are turned on, the target surface becomes coated with thin films of fluorocarbon or hydrocarbon and so the measurements are not on pristine surfaces. This might not meet with the approval of a Ph. D. thesis examiner, but probably provides more useful information than an experiment performed on pure Al. Sugai et al find that at low energies most of the ions are neutralized upon impact. They study the probability of dissociation among the reflected ions, but unfortunately do not detect the reflected neutrals, which are more numerous. Once again, the difficulty of observing neutral products is retarding progress, as it has with respect to electron impact reactions.

Plasma Cleaning

Control over semiconductor processing requires frequent cleaning, for the reactor itself between wafers as well as for the wafers before or after each processing step. Two problems of special interest are the removal of deposits from reactor walls and the removal of the resists that are used in lithography from the semiconductor wafers. In deposition systems some of the feedstock gas can be deposited on the reactor walls instead of the work-piece, while in etching the wall deposits can either be etch products or the polymer layers that are used for passivation on the substrate. Photoresist mask materials are primarily long-chain organic polymers consisting mostly of hydrogen and carbon or, in the so-called hard masks, are composed of Si_3N_4 or SiO_2.

Plasma cleaning differs from plasma etching in that the process can be isotropic, but selectivity is still important to avoid damage to the work-piece or reactor. The process is also known as ashing or stripping.

Although the details of cleaning techniques vary with the primary process, the type of reactor, the gas mixture and the wall material, the basic idea is to deliver low energy etching radicals, such as F or O atoms to the surface. Typical sources of these radicals are O_2, NF_3, SF_6, C_xF_y, CF_4/O_2 and CF_4/H_2O, often mixed with rare gases or N_2 to ease plasma formation.

The radicals have traditionally been created in situ by creating a relatively quiet plasma that will do minimal damage to the system. There is growing interest in the use of downstream systems, in which the radicals are created in a separate discharge and are transported to the reactor. Clearly it is important to minimize radical recombination, either in the gas phase or on surfaces, as the gas moves from the source to the processing chamber. A data set for downstream etching in an NF_3/O_2 mix has been given by Meeks et al. (84)

As feature sizes shrink, there is growing concern about the deleterious effects of ions on semiconductor devices. Not only can energetic ions cause collateral damage, but the charging of dielectric surfaces can perturb the trajectories of electrons and ions that arrive later or can cause shorting. Thus all opportunities to perform dry chemistry using radical rather than ions are being sought, with the radicals being formed in a remote reactor (85,86).

Data Needs

A survey of data needs for the semiconductor manufacturing industry was carried out recently under the auspices of the U. S. National Research Council and their report was published in 1996 (87). This report covers structural, radiative and collisional processes in both the gas phase and on surfaces. With respect to the assembly of data on electron collisions, two promising developments since that time have been the series of articles by Christophorou, Olthoff and Rao (88) on CF_4, CHF_3, CCl_2F_2 and C_2F_6, and the internet site maintained by Kinema Research (89). The review by Oehrlein (90) provides a valuable supplement to the NRC report in regard to surface reactions.

Although the nature of the required data varies from one application to the next, a common need is to understand all the processes that govern the creation, transformation and destruction of radicals and ions. Most of the molecules that make up the plasma are created by reactions, either in the discharge or on surfaces, and the effects of reaction products on charge and energy balance and on particle transport must be considered. Excitations leading to metastable states are almost always significant, and accurate data on those specific excitations that lead to diagnostic radiation are especially valuable.

POLLUTION CONTROL

Plasma techniques for treating hazardous gases are usually divided into two classes, thermal and non-thermal methods. In the thermal approach, the applied electrical power is mostly used to heat the gas to a temperature at which the chemical reactions lead to the destruction of the unwanted species. These methods draw less on physical data and are not discussed here.

Non-thermal plasma processing operates by producing a plasma in which the majority of the electrical energy goes into the production of energetic electrons. These plasmas are characterized by electrons with kinetic energies much higher than those of the ions or molecules. Even though the electrons are short-lived under atmospheric conditions and collide relatively rarely with the pollutant molecules, they undergo many collisions with the dominant bulk-gas molecules. Electron-impact dissociation and ionization of the background gas molecules create a mix of reactive species, in the form of radicals, ions and secondary electrons, that permits unique and diverse chemical reactions to be possible even at relatively low temperatures. The potential of the approach to gas cleanup arises from the fact that these species react selectively with the pollutant molecules, which are often present in very small concentrations.

Non-thermal plasmas can be formed using electron beams or electrical discharges. In the electron beam method, electrons are accelerated by high voltage in a vacuum region before being injected through a thin foil window that serves as a vacuum seal The high-energy electrons going through the thin window can then be used to produce a large volume of plasma as they collide with the gas molecules in an atmospheric-pressure processing chamber.

In the electrical discharge method, the high voltage electrodes are immersed in the atmospheric-pressure gas, instead of a vacuum. The electrons collide with and transfer energy to the gas molecules as they drift along the high voltage region. The electrical discharge method therefore results in average electron energies less than those obtained from the electron beam method. The numbers of secondary electrons, ions and reactive free radicals are strongly influenced by the electron energy distribution. A comparison of the relative efficiencies of the two approaches for four volatile organic compounds (ethylene, o-xylene, toluene and benzene) has been given by Penetrante et al. (91).

The two major issues facing the commercial implementation of non-thermal plasmas to pollution control are the process efficiency and the identity of the byproducts (92).

For example, systems to treat the exhausts from engines or power plants will usually be of little interest if they consume more than 10% of the generated power or produce molecules that are more hazardous than those being removed. There are two kinds of efficiencies of concern: (a) electrical conversion efficiency, and (b) chemical processing efficiency. The electrical conversion efficiency refers to the efficiency for converting wall plug electrical power into power deposited by the electrons into the plasma. The chemical processing efficiency refers to the amount of pollutant removed or decomposed for a given amount of energy deposited into the plasma. The chemical processing efficiency is often expressed in terms of the specific energy consumption in units such as eV per pollutant molecule, or grams of pollutant per kW-hr. The electrical conversion efficiency is highly dependent on the plasma reactor configuration and power supply used, and so will not be discussed here. On the other hand, the chemical processing efficiency is a more basic quantity, making it possible (under the same gas conditions) to compare the radical, ion or electron production in different reactors regardless of the reactor configuration or power supply.

It is often difficult to assess and compare the performance of various kinds of plasma reactors. The data presented in the literature using different kinds of reactors often were measured under different gas conditions. In many cases, the data are presented in a way that makes it impossible for the reader to determine the energy consumption of the reactor.

In this section we will examine typical processes by which non-thermal plasmas can treat various gas phase pollutants. The kinetic analysis of the deposition of energy into contaminated air will be reviewed. The collisions of electrons with the air molecules result in the formation of ions, secondary electrons and reactive free radicals. The role of these plasma species in the decomposition of various pollutant molecules will be illustrated by studies of the removal of nitrogen oxides (NO_x), methylene chloride, carbon tetrachloride, methanol and trichloroethylene. A more detailed review of the kinetics has been presented by Penetrante et al (93).

Energy Deposition

The intent in using a non-thermal plasma is to selectively transfer the input electrical energy to the electrons. In the kinetic analysis of non-thermal plasma methods, the first step is to understand the deposition of energy into contaminated air. This is controlled primarily by the major components, N_2 and O_2. Because of the resonance in electron scattering by N_2 near 2 eV, low energy electrons lose considerable energy through vibrational excitation (94, 95) which does little to enhance the desired reactions. Thus raising the average electron energy well above 2 eV is necessary for efficient treatment.

The most useful energy deposition into N_2 and O_2 is usually associated with the production of N and O atoms through electron impact dissociation (96,97) and ionization (94,95), producing either atomic or molecular ions. One must also account for the creation of metastables, especially in the dissociated atoms O and N. For

example, the reaction rates for the metastable $O(^1D)$ are almost always larger than those for the corresponding reactions with ground state $O(^3P)$ (98-100). This can enhance both desired and undesired reactions. Detailed analyses of electron transport and electron excitation processes in N_2-O_2 discharges have been given recently by Guerra et al. (101) and by Slavik and Colonna (102).

The electron energy distribution in a plasma reactor is important because it determines the types of radicals produced in the plasma and the input electrical energy required to produce those radicals. In discharge processing, the rate coefficients for electron-impact dissociation reactions strongly depend on the electron mean energy in the discharge plasma. In coronal discharges, the non-thermal plasma is produced through the formation of statistically distributed microdischarges known as streamers (103-107). The electrons dissociate and ionize the background gas molecules within nanoseconds in the narrow channel formed by each microdischarge. The electron energy distribution in the plasma is complicated because the electric field is strongly non-uniform (e.g. because of strong space-charge field effects) and time dependent. During the microdischarge formation phase, the electron number rises drastically. Due to field strength enhancement in the ionization wave, the highest electron energies occur during this phase. The mean electron energy reaches values of more than 10 eV - suitable for considerable dissociation and ionization of the gas. However, since this is a highly transient phase, and since the ionization wave covers only small parts of the gap at any one time, this phase may be less important in producing most of the active radicals.

The Livermore group (93) believes that most of the species responsible for the chemical processing are generated during the main current flow in established microdischarge channels. Other authors (106,107) believe that most of the active species are produced in the strong field regions near the tip. This is an important issue, not just a debating point between theorists. If the number of ions and radicals depends critically on the maximum strength of the electric field in the streamer tip, there should be scope for innovative devices to optimize the pulsed power system that drives the streamers. On the other hand, if the average field strength is more important, there is little to be gained by complex electrode geometries or pulse shapes. The Livermore group believes that the electrical engineers should concentrate more on the wall-plug efficiency of the power system and the lifetime and cost of the device than on tailoring the system to increase the electric field in the streamer tip.

The dissipation of input electrical power as a function of the average kinetic energy of the electrons in a dry air discharge is shown in Figure 5. The electron mean energy in most electrical discharge reactors operating at atmospheric pressure is typically between 3 and 6 eV. In this range, a large fraction of the input power is wasted in vibrational excitation of N_2 and a significant fraction goes into dissociation of O_2. The electron mean energy in electrical discharge reactors is optimal for the electron-impact dissociation of O_2, which is important for the production of O radicals. These oxidizing radicals play a key role in the generation of ozone (108-110). However, for reaction chains that are initiated by dissociation of N_2 or by the creation of ion pairs,

the higher energies obtained in the electron beam method usually lead to higher chemical efficiencies. More detailed comparisons of energy deposition mechanisms in electron beam and coronal discharge plasmas can be found elsewhere (92,93,111).

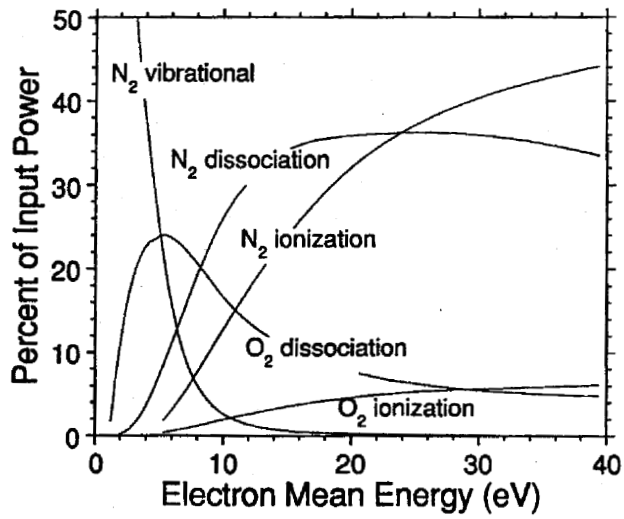

FIGURE 5. Electrical power deposition in a dry air discharge showing the percentage of input power consumed in various electron-impact processes (Courtesy: B. M. Penetrante).

In humid air mixtures (112,113), OH radicals can be produced in a variety of ways. In discharge reactors for which the electron mean energy is low, the OH radicals are produced via three types of reactions:

electron attachment:

$$e + H_2O \rightarrow H^- + OH \quad (1)$$

direct dissociation by electron impact:

$$e + H_2O \rightarrow e + H + OH \quad (2)$$

dissociation by $O(^1D)$:

$$O(^1D) + H_2O \rightarrow 2\ OH \quad (3)$$

In electron beam reactors, the OH radicals come mainly from the positive ions reacting with H_2O. The sequence of fast steps are as follows:

electron-impact ionization:

$$e + O_2 \rightarrow 2e + O_2^+ \quad (4)$$

and similar ionization processes to produce molecular ions N_2^+, H_2O^+, CO_2^+

electron-impact dissociative ionization:

$$e + O_2 \rightarrow 2e + O + O^+ \quad (5)$$

and similar dissociative ionization processes to produce N^+, H^+

charge transfer reactions to form additional O_2^+ ions, such as:

$$N_2^+ + O_2 \rightarrow N_2 + O_2^+ \quad (6)$$

formation of water cluster ions:

$$O_2^+ + H_2O + M \rightarrow O_2^+ (H_2O) + M \quad (7)$$

dissociative reactions of water cluster ions to form OH:

$$O_2^+ (H_2O) + H_2O \rightarrow H_3O^+ + O_2 + OH \quad (8)$$

$$O_2^+ (H_2O) + H_2O \rightarrow H_3O^+ (OH) + O_2 \quad (9)$$

followed by

$$H_3O^+ (OH) + H_2 \rightarrow H_3O^+ + H_2O + OH \quad (10)$$

Benchmark Experiments

The kinetics of pollution control systems are usually extremely complex, involving tens of species and hundreds of reactions, and the data on reaction rates is incomplete. Thus it is important to carry out simplified experiments, in which the number of components is limited. For example, studies of NO removal in pure N_2 (114) have helped to check the data on energy deposition in N_2 and the reduction of NO through the reaction

$$N + NO \rightarrow N_2 + O \quad (11)$$

It must be stressed that simplified experiments of this kind are valuable only for checking reaction rate data and not as direct indicators of what happens in real systems. To complete the analysis of NO removal from exhaust gases, it is necessary to account for the effects of other gas-phase constituents, such as O_2, CO_2 and H_2O, the gas temperature, and surface reactions on particulates as well as chamber walls.

For very dilute concentrations of NO in N_2, the input energy required for NO reduction is determined by the energy required for dissociation of N_2. The input electrical energy is consumed in electron-impact reactions with N_2 and the removal of NO proceeds mainly via reduction by the N atom. By doing experiments using this mixture it is therefore possible to examine the dependence of the dissociation rate of N_2 on the different types of plasma reactors. These experiments (114) also provide a validation of the calculated N_2 dissociation rates.

Penetrante et al (115) presented a systematic comparison of data on plasma-induced NO reduction obtained from three different laboratories using independently constructed discharge reactors and different chemical diagnostic methods. By using identical gas mixtures, the plasma processing performance of various reactors could be compared. The important control parameter is the energy density input, which is the power input into the gas divided by the total gas flow rate. The concentration of NO (in units of parts per million) as a function of the input energy density (in units of Joules per standard liter) is shown in Figure 6. The six coronal reactors used a wide variety of electrode materials, geometries and power supplies, but showed very similar chemical efficiencies. The specific energy cost for NO reduction using the various electrical discharge reactors ranged from 0.8 to 1.25 ppm-liters/Joule.

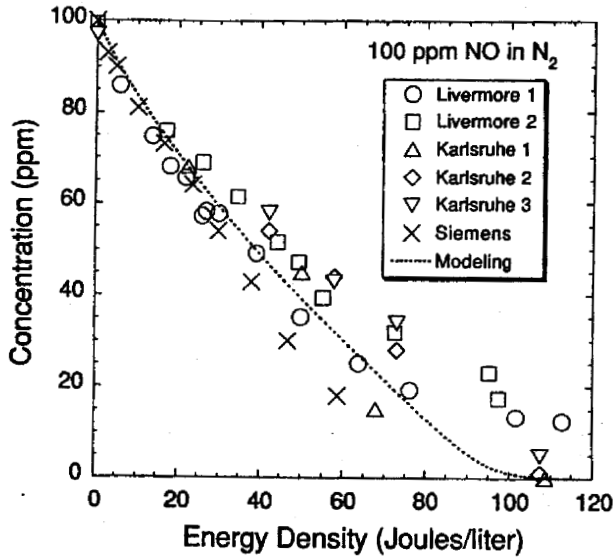

FIGURE 6. The destruction of NO molecules as a function of deposited energy in pulsed corona and dielectric-barrier discharges, beginning with 100 ppm NO in N_2 at atmospheric pressure.

The dotted line in Figure 6 shows the results of models using the cross sections for electron impact dissociation of N_2 as measured by Cosby (97). The agreement is much poorer when the cross sections of Winters (96) are used. It would be very useful if a third experimental measurement could be made to determine which measurement is correct.

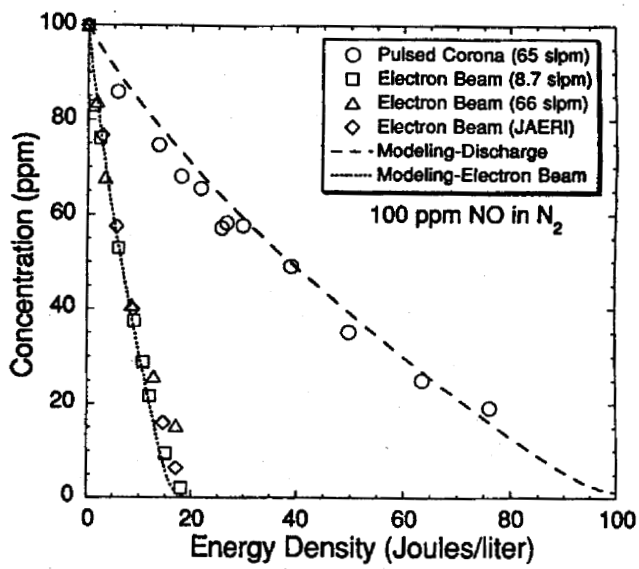

FIGURE 7. Electron beam and pulsed corona processing of 100 ppm NO in N_2.

In figure 7, these results obtained with pulsed corona are compared with those obtained in three electron beam experiments and with models using the same cross

section set. Full details can be found in the paper by Penetrante et al (93). The greater efficiency of NO destruction in the electron beam experiments is due to the larger dissociation rates that arise from the higher average electron energy.

Reaction Mechanisms

When small amounts of NO are destroyed in N_2 discharges, the process is reductive, leading to N_2 and O_2, driven by reaction (11). However, in the presence of O_2, the removal process is primarily oxidative (116), driven by the reaction

$$O + NO + M \rightarrow NO_2 + M. \quad (12)$$

In the presence of water, acids are usually formed through reactions like

$$OH + NO_2 + M \rightarrow HNO_3 + M. \quad (13)$$

The presence of water droplets can introduce surface reactions, which must be taken into account (117). In stationary applications, such as power plants burning fossil fuel (118,119) and automobile tunnels, these acids can be neutralized, for example through the addition of ammonia (120) to form phosphates. These can be sold as fertilizer, if they are not contaminated with toxic by-products. Since the easiest way to remove NO is to turn it into other oxides of nitrogen, it is important not to base analyses purely on the disappearance of NO.

Much of the research into non-thermal treatment of gaseous pollutants has been focused upon volatile organic compounds. An excellent review of this work has been given by Vercammen et al. (121). A major concern is with chlorinated carbon and hydrocarbon compounds, which are widely used as industrial solvents and are often found in hazardous concentrations at government and industrial cleanup sites. For example, methylene chloride (CH_2Cl_2) is used for removing paint from aircraft. An examination of the rate coefficients for methylene chloride decomposition in a non-thermal plasma (122) show that the most likely mechanism is the reaction with nitrogen atoms

$$N + CH_2Cl_2 \rightarrow \text{products} \quad (14)$$

If the decomposition of methylene chloride is dominated by reaction (14), we would expect that, for the same initial concentrations, the energy consumption for processing methylene chloride in N_2 should be the same as the energy consumption for processing NO in N_2. The rate controlling step is the production of N atoms. This has been verified experimentally (122), as shown in Figure 8. Deviations between methylene chloride and NO are observed only after the concentration has dropped down to around 15 ppm. This deviation may be caused by the consumption of N atoms in reactions with the intermediate products during the decomposition of methylene chloride. The destruction of methylene chloride in discharge reactors becomes much more efficient if the temperature is raised to 300C (122,123).

In dry air, methanol is primarily destroyed (124) by ions, through the dissociative charge transfer reaction

$$N_2^+ + CH_3OH \rightarrow CH_3^+ + OH + N_2 \quad (15)$$

Additional reactions may result from the formation of OH radicals from the initial decomposition reaction (15). Comparison of the decomposition rates in pure nitrogen and dry air suggests that O radicals are not particularly efficient at destroying methanol.

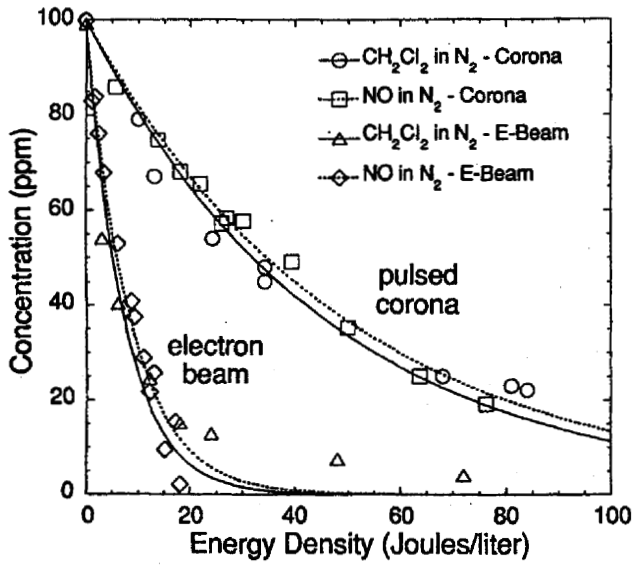

FIGURE 8. Comparison of the destruction rates of NO and methylene chloride in electron beam and pulsed corona reactors.

Examination of the rate coefficients for carbon tetrachloride decomposition in a non-thermal plasma (125-128) show that the rate limiting step is the dissociative attachment of carbon tetrachloride to secondary electrons

$$e + CCl_4 \rightarrow Cl^- + Cl_3 \qquad (16)$$

Since an electron-ion pair is produced during an ionization event, the energy consumption for producing electrons should be the same as that for producing ions. In the case of carbon tetrachloride, the electrons do the decomposition. In the case of methanol, the positive ions are the prime agent. Experiments (124,125) show that the energy required to consumption to destroy carbon tetrachloride in dry air is the same as that for decomposing methanol. This suggests that the rate limiting step is electron-ion pair formation in methanol as well as in CCl_4.

There has been significant recent progress (129-131) in understanding the complex reaction chain responsible for the destruction of trichloroethylene (TCE or C_2HCl_3). At least in the electron-beam treatment, the initial reaction appears to be electron impact dissociative attachment

$$e + C_2HCl_3 \rightarrow Cl^- + C_2HCl_2 \qquad (17)$$

In discharge processing, the electron density is lower and TCE can also be broken up by attacks from O, OH or O_3 upon the C=C double bond (92,129,130). The observation that the rate of destruction increases as the removal proceeds has led to the conclusion that there must be an autocatalytic process, involving a chain of reactions

initiated by Cl radicals, that not only destroys one TCE molecule, but also creates several new Cl radicals.

Analysis of the by-products is extremely important in pollution treatment. Two products that may arise from the destruction of chlorinated hydrocarbons are phosgene ($COCl_2$) and dichloroacetyl chloride (DCAC or $CHCl_2COCl$). Although phosgene is extremely toxic, it can be easily removed by bubbling through water.

Scavenging Reactions

Not all reactions of radicals or ions are beneficial. For example, the three-body reaction

$$Cl + CCl_3 + M \rightarrow CCl_4 + M \quad (18)$$

destroys two radicals and recreates the unwanted molecule. Fortunately, the presence of O_2 scavenges the CCl_3 through the fast reaction

$$CCl_3 + O_2 \rightarrow CCl_3O_2 \quad (19)$$

Scavenging reactions can also be detrimental. For example, electrons can be removed through attachment to O_2 or H_2O rather than to CCl_4. After the concentration of CCl_4 has decreased to a few tens of ppm, the three-body attachment of secondary electrons to oxygen molecules

$$e + O_2 + O_2 \rightarrow O_2^- + O_2 \quad (20)$$

$$e + O_2 + N_2 \rightarrow O_2^- + N_2 \quad (21)$$

becomes a significant electron loss pathway compared to reaction (16). The attachment frequency of secondary electrons to O_2 in dry air at atmospheric pressure is

$$\nu_{O2} = k_{(20)} [O_2]^2 + k_{(21)} [N_2] [O_2] \text{ Å } 0.8\text{x}10^8 \text{ s}^{-1}. \quad (22)$$

For 100 ppm CCl_4, the attachment frequency to CCl_4 is

$$\nu_{CCl4} = k_{(17)} [CCl_4] \text{ Å } 10^9 \text{ s}^{-1}. \quad (23)$$

When the concentration of CCl_4 is down to around 10 ppm, the electrons will attach to oxygen molecules as frequently as to CCl_4 molecules.

Humidity enhances the attachment of electrons to O_2 via

$$e + O_2 + H_2O \rightarrow O_2^- + H_2O \quad (24)$$

In humid air, the attachment frequency of secondary electrons to O_2 is

$$\nu_{O2} = k_{(20)} [O_2]^2 + k_{(21)} [N_2] [O_2] + k_{(24)} [H_2O] [O_2] \text{ Å } 1.5\text{x}10^8 \text{ s}^{-1}. \quad (25)$$

Figure 9 compares the results of experiments on electron beam processing of 100 ppm of CCl_4 in dry air and humid air. Note that humidity is deleterious to the decomposition of CCl_4. Humidity enhances the attachment of electrons to O_2, thus effectively decreasing the efficiency for decomposition of CCl_4.

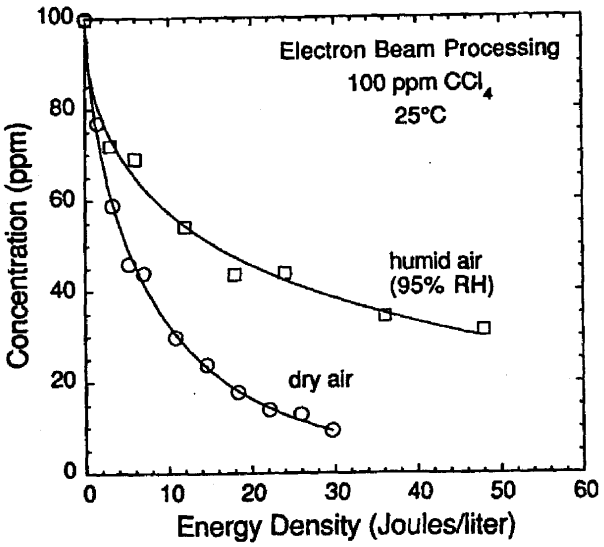

FIGURE 9. Electron beam processing of 100 ppm CCl_4 in dry air and humid air at atmospheric pressure.

Effect of Excited Species

The amount of NO reduction is directly proportional to the number of N_2 dissociations that can be achieved in the plasma. Unfortunately, not all of the N atoms resulting from the dissociation of N_2 lead to the reduction of NO. Dissociative excitation of N_2 contributes a large fraction to the total N_2 dissociation (131). A significant species produced by dissociative excitation of N_2 is the long-lived metastable, $N(^2D)$. For electron beam reactors, over half of the total N radicals produced are in the excited metastable states. The rate constants characterizing the interaction of the metastable species $N(^2D)$ with various gases are large In the treatment of NO, there are two competing reactions involving the $N(^2D)$ metastable species:

$$N(^2D) + NO \rightarrow N_2 + O \quad (26)$$

$$N(^2D) + O_2 \rightarrow NO + O \quad (27)$$

With 1000 ppm NO and 10% O_2 , the $N(^2D)$ species is ten times more likely to react with O_2 than with NO. This means that $N(^2D)$ is consumed in the production of NO rather than in the reduction of NO. Whereas the reaction of ground state N atoms, $N(^4S)$, with O_2 can proceed only at very high temperatures, the reaction of excited N atoms, $N(^2D)$, with O_2 can proceed even at room temperature. Since almost half of the total N atoms produced in the plasma are in this excited state, the reduction of NO by the ground state N atoms is almost completely counterbalanced by the production of

NO by the excited N atoms. What is left in terms of NO reactions is the oxidation reaction (12)

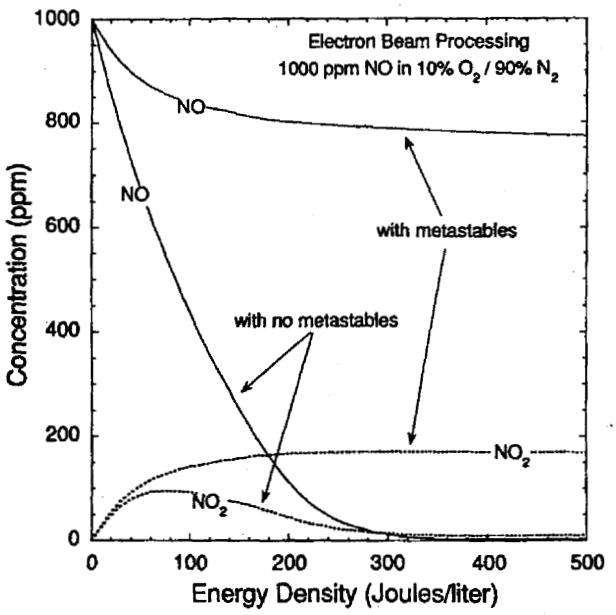

FIGURE 10. Calculations showing the effect of $N(^2D)$ metastable atoms on electron beam processing of 1000 ppm NO in a 90% N_2/ 10% O_2 mixture at atmospheric pressure.

Calculations showing the effect of the metastable species $N(^2D)$ on electron beam processing of 1000 ppm NO in a 90% N_2 /10% O_2 mixture is shown in Figure 10. The agreement between these results and experiments (143) at the Japan Atomic Energy Research Institute (JAERI) on electron beam processing of 500 ppm NO in 97% N_2/3% O_2 provides support for the thesis that $N(^2D)$ is responsible for the deleterious effect of O_2 in electron beam processing.

Catalytic Surface Reactions

Despite the progress that has been made over the past decade, the economics of pollution control using coronal discharges seems marginal at best and their is little incentive to chemical engineers to adopt a new technology. The prime approach to cost-effective chemical processing is to use catalytic reactions (132) and so there is growing interest in the combination of plasma techniques and catalysis. Removing NO_x from diesel engines and lean-burn gasoline engines is a particularly attractive target for such work, since the catalysts that work so well for automobile engines are quickly poisoned due to the added oxygen and water content of the diesel exhaust.

One of the first approaches to combine plasma and surface reactions was through the use of a packed bed reactor (133,134), in which pellets are used both to enhance

the electric fields and to provide surfaces for heterogeneous reactions. Unfortunately, this work has become so sensitive that unsuccessful attempts are published (135), whereas more successful ones are not. Billions of dollars are at stake! Once again, the paucity of data concerning the interactions of plasmas with real (far from pristine) surfaces is seriously hampering research.

Further Data Needs

By understanding what plasma species is responsible for the decomposition of a pollutant molecule, it is possible to establish the electrical power requirements of the plasma reactor and help identify the initial reactions that lead to the subsequent process chemistry. There is much work still to be done in understanding the full chemical kinetics for many pollutant molecules. Nevertheless, the kinetics with respect to electron-impact reactions can been studied thoroughly enough so that it is possible to identify which plasma component (electron, positive ion, nitrogen atom or oxygen radical) is mainly responsible for the initial decomposition of various pollutant molecules. The effort to assemble and assess data on the neutral reactions in the atmosphere (99,100,136) is also very useful in understanding the susequent chemistry. It would be helpful if the data sets on atmospheric ion-molecule reactions could also be updated.

Although the execution of benchmark experiments and the development of complex reaction schemes have led to considerable progress in understanding the kinetics for relatively simple gas-phase systems, much more work is needed on the effects of minor constituents in the exhaust, surface reactions and temperature variations. Determination of the energy efficiency, by-products and scalability of the treatment process are critical to the commercial success of this technology, and detailed understanding of the underlying science will help in each respect.

CONCLUSIONS

Almost all industrial plasmas are unconfined. This means that for neutral atoms and molecules or ions, collisions with surfaces are at least as important, and often more important, than gas phase collisions. For electrons, collisions within the plasma are more significant, since the approach of electrons to the walls is usually retarded by the plasma potential. Thus electron impact dissociation of molecules is usually balanced by association on surfaces. On the other hand, electron impact ionization is often balanced mainly by gas-phase recombination, either through dissociative recombination or ion-ion reactions.

The major need for data currently is in support of computer simulations of industrial processes. These are usually used for off-line analysis and in support of empirical development of new processes and new equipment. When databases are more complete and simulations more accurate, it will become possible to use plasma

diagnostics for real-time control of plasma processing and for computer-aided design in process development (137). This could lead to significant savings in time and expense, but has not yet been achieved in most industrial applications of plasmas.

The list of species and processes in this review is by no means complete, but shows the need for much work by the atomic, molecular and optical physics community. One characteristic is perhaps worthy of mention. The atoms and molecules that are listed here are not the easiest for academic study, either experimentally or theoretically. The industrial interest often arises because the gases are reactive and therefore nasty to handle, in one way or other. Thus there is often a need to know the details of a particular process that has been studied by researchers for other, more benign, species. It is then very difficult for academics to obtain funds to make the appropriate measurement or calculation. It is essential that government, academia and industry continue to work together to identify those processes that are of paramount importance and to provide support for the generation, assembly and dissemination of the necessary data.

ACKNOWLEDGEMENTS

This work was performed under the auspices of the U.S. Department of Energy by the University of California, Lawrence Livermore National Laboratory under Contract No. W-7405-Eng-48.

and partly at the U. S. Display Consortium with support from the Defense Advanced Projects Agency. The author is grateful for the assistance of many of his colleagues in the preparation of this manuscript, particularly to Bernie Penetrante, Jong Shon and Peter Vitello.

REFERENCES

1. Siemens, W., *Ann. Phys. Chem.* **102**, 66-122 (1857).
2. Hittorf, W., *Ann. Physik* **21**, 90-139 (1884).
3. Thomson, J. J., *Phil. Mag.* **32**, 321-36,445-64 (1891).
4. "Tesla's experiments with alternating current at high frequency", *Electrical Engineer*, **7**, 549-50 (1891).
5. Wharmby, D. O., "Electrodeless lamps for lighting", *IEE Proceedings A* **140**, 465-73 (1993).
6. Work,D.E., *Light. Res. Technol.* **13**, 143 (1981).
7. Dakin, J. T., Rautenburg, T. H., and Goldfield, E. M., *J. Appl. Phys.* **66**, 4074-88 (1989).
8. Shaffner, R. O., "Prime Color Light Source Development for Helmet Mounted Displays" in *SPIE Proceedings* **2735**, 136-40 (1996).
9. Kogelschatz, U., Eliasson, B., and Egli, W., *J. Physique IV* **7**, Colloque C4, 47-66 (1997).

10. Kogelschatz, U., *Appl. Surf. Sci.* 54, 410-23 (1992).
11. Rosocha, L. A., "Processing of hazardous chemicals using silent-discharge plasmas", in *Plasma Science and the Environment*, (eds. Mannheimer, W., Sugiyama, L. E. ,Stix, T. H., AIP, New York, 1997) pp. 261-98.
12. Ilcisin, K. J., Buzak, T. S., and Parker, G. J., *J. Physique IV* 7, Colloque C4, 225-34 (1997).
13. Ilcisin, K., Buzak, T., Hinchliffe, R., Martin P., Roberson, M., Kakizaki, T., Tanamachi, S., Hayashi, M. amd Morita T., "Breakthrough gas mixtures for HDTV performance in plasma addressed displays", in *Eurodisplay 96* (Society of Information Display, 1996) pp 595-99.
14. Boeuf, J.-P., Punset, C., Hirech, A. and Doyeux, H., *J. Physique IV* 7, Colloque C4, 3-14 (1997).
15. Punset, C., Boeuf, J.-P., and Pitchford, L. C., *J. Appl. Phys.* **83**, 1884-97 (1998).
16. Veerasingham, R., Campbell, R. B., and McGrath, R. T., *IEEE Trans. Plasma Sci.* **24**, 1411 (1996).
17. Choi, K. C., and Whang, K. W., *IEEEE Trans. Plasma Sci.* **23**, 399-404 (1995).
18. Fiala, A., Pitchford, L. C., and Boeuf, J.-P., *Phys. Rev E* **49**, 5607-22 (1994).
19. Veerasingham, R., Campbell, R. B., and McGrath, R. T., *Plasma Sources Sci. Technol.* **6**, 157-169 (1997).
20. Falkenstein, Z., and Coogan, J. J., *J. Phys. D* **30**, 2704-10 (1997).
21. Meunier, J, Belanguer, P., and Boeuf, J. -P., *J. Appl. Phys.* **78** 731-45 (1995).
22. Boeuf, J.-P., and Pitchford, L. C., *IEEE Trans. Plasma Sci.* **24**, 95 (1996).
23. Tachibana, K. Kosugi, N., Sakai, T., *Appl. Phys. Lett.* **65**, 935-7 (1994).
24. Lieberman, M. A. and Lichtenberg, A. J., *"Principles of Plasma Discharges and Materials Processing"*, New York: John Wiley, 1994.
25. Ricard, A., *J. Phys. D.* **30**, 2261-9 (1997).
26. Baldwin, M. J., Collins, G. A., Fewell, M. P., Haydon, S. C., Kumar, S., Short, K. T., and Tendys, J., *Jpn. J. Appl. Phys.* **36**, 4941-8 (1997).
27. Jones, E. C., Shao, J.,Denholm, A. S., and Cheung, N. W., *Jpn. J. Phys.* **36**, 4935-40 (1997).
28. Keller, J. H., Forster, J. C., and Barnes, M. S., *J. Vac. Sci. Technol. A.* **11**, 2487 (1993); Barnes, M. S., Forster, J. C., and Keller, J. H., *Appl. Phys Lett.* **62**, 2622 (1993).
29. Carter, J. B., Holland, J. P., Peltzer, E., Richardson, B., Bogle, E., Nguyen, H. T., Melaku, Y., Gates, D., and Ben-Dor, M., ., *J. Vac. Sci. Technol. B.* **11**, 1301 (1993).
30. Asmussen, J., Grotjohn, T. A., and Perrin, M. A., *IEEE Trans. Plasma Sci.* **25**, 1196-221 (1997).
31. Chen, F. F. and Boswell, R. W., *IEEE Trans. Plasma Sci.* **25**, 1245-57 (1997).
32. Yoshimura, K., Miki, T., and Tanemura, S., *J. Vac. Sci. Technol. A.* **15**, 2673-6 (1997).
33. Nakashima, H., Furukawa, K. Liu, Y. C., Gao, D. W. Kashiwakazi, Y., Muraoka, K., Shibata, K., and Tsurushima, T., *J. Vac. Sci. Technol. A.* **15**, 1951-4 (1997).

34. McCormick, C. S., Weber, C. E., Abelson, J. R., Davis, G. A., Weiss, R. E., and Aebi, V., *J. Vac. Sci. Technol. A.* **15**, 2770-6 (1997).
35. Hopwood, J. and Qian, F., *J. Appl. Phys.* **78**, 758-65 (1995).
36. Dickson, M., and Hopwood, J., *J. Vac. Sci. Technol. A.* **15**, 2307-12 (1997).
37. Leroy, O., Jolly, J., and Perrin, J., "2D Electrical, thermal and chemical modeling and diagnostics of SiH_4-H_2 RF discharges", *Proceedings of the 3rd Int. Conf. on Reactive Plasmas*, Nara, January 1997, pp. 13-4.
38. Leroy, O., Dorval, N., Hertl, M., Jolly, J., and Pealat, M., "Theoretical and experimental study of SiH radical density and thin film growth in PECVD H_2/SiH_4 radio frequency discharges", in *Proceedings of the 23rd Int. Conf. on Phenomena in Ionized Gases, Vol IV,* Toulouse, July 1997, pp. 216-7.
39. Perrin, J., Leroy, O., and Bordage, M. C., *Contrib. Plasma Phys.* **36,** 3-49 (1996).
40. Perrin, J., Shiritani, M., Kae-Nune, P., Videlot, H., Jolly, J., and Guillon, J., *J. Vac. Sci. Technol. A.* **16**, 278-89 (1998).
41. Kawasaki, H., Ohkura, H., Fukuzawa, T., Shiritani, M., Watanabe, Y., Yamamoto, Y., Suganuma, S., Hori, M., and Goto, T., *Jpn. J. Appl. Phys.* **36,** 4985-8 (1997).
42. Kim, D.-J., and Kim, K.-S., *Jpn. J. Appl. Phys.* **36,** 4989-96 (1997).
43. Childs, M. A., and Gallagher, A., *Bull. Amer. Phys. Soc.* **42**, No 8,1733 (1997).
44. Hugon, M. C., Delmotte, F., Agius, B., and Courant, J. L., *J. Vac. Sci. Technol. A.* **15**, 3143-53 (1997).
45. Delmotte, F., Hugon, M. C., Agius, B., and Courant, J. L., *J. Vac. Sci. Technol. B.* **15**, 1919-26 (1997).
46. Caquineau, H., Dupont, G., Despax, B., and Couderc, J. P., *J. Vac. Sci. Technol. A* **14**, 2071-82 (1996).
47. Meeks, E., Larson, R. S., Ho, P., Apblett, C., Han, S. M., Edelberg, E., Aydil, E. S., *J. Vac. Sci. Technol. A.* **16**, 544-63 (1998).
48. Gaillard, F., Brault, P., and Broquet, P., *J. Vac. Sci. Technol. A.* **15**, 2478-84 (1997).
49. Fracassi, F., d'Agostino, R., and Favia, P., *J. Electrochem. Soc.* **139**, 2636-44 (1992).
50. Basner, R., Foest, R., Schmidt, M., Hempel, F., and Becker, K., "Ions and Neutrals in the Ar-TEOS RF Discharge", in *Proceedings of the 23rd Int. Conf. on Phenomena in Ionized Gases, Vol IV,* Toulouse, July 1997, pp. 196-7.
51. Han, S. M. and Aydil, E. S., *J. Vac. Sci. Technol. A.* **15**, 2893-904 (1997).
52. Yoshimaru, M., Koizumi, S., and Shimokawa, K., *J. Vac. Sci. Technol. A.* **15**, 2908-14, 2915-22 (1997).
53. Tennant, D., Klemens, F., Sorsch, T., Baumann, F., Timp, G., Layadi, N., Kornblit, A., Sapjeta, B. J., Rosamilia, J., Boone, T., Weir, B., and Silverman, P., *J. Vac. Sci. Technol. B.* **15**, 2799-805 (1997).
54. Richter, H. H., Aminpur, M.-A., Erzgraber, H. B., Wolff, A., Kruger, D., Dehoff, A., and Reetz, M., *Jpn. J. Appl. Phys.* **36**, 4649-53 (1997).
55. Nishikawa, K., Ono, K., Tuda, M., Oomori, T., and Namba, K., *Jpn. J. Appl. Phys.* **34**, 3731-6 (1995).

56. Choe, J. Y. Herman, I. P., and Donnelly, V. M., *J. Vac. Sci. Technol. A* **15**, 3024-31 (1997).
57. Kota, G. P., Coburn, J. W., and Graves, D. B., *J. Vac. Sci. Technol. A.* **16**, 270-7 (1998).
58. Chang, J. P., Arnold, J. C., Zau, G. C. H., Shin, H.-S., and Sawin, H. H. *J. Vac. Sci. Technol. A* **15**, 1853-63 (1997).
59. Chang, J. P., Mahorowala, A. P., and Sawin, H. H., *J. Vac. Sci. Technol. A.* **16**, 217-24 (1998).
60. Levinson, J. A., Shaqfeh, E. S. G., Balooch, M., and Hamza, A. V., *J. Vac. Sci. Technol. A* **15**, 1902-12 (1997).
61. Ono, K., and Tuda, M., *Jpn. J. Appl. Phys.* **36** 4854-65 (1997).
62. Doshita, H., Ohtani, K., and Namiki, A., *J. Vac. Sci. Technol.A.* **16**, 265-9 (1998).
63. Layadi, N., Donnelly, V. M, and Lee, J. T. C., *J. Appl. Phys.* **81**, 6738-48 (1997).
64. Donnelly, V. M., *J. Vac. Sci. Technol. A* **14**, 1076-87 (1996).
65. Ono K., Tuda, M., Nishikawa, K., Oomori, T., and Namba, K., *Jpn. J. Appl. Phys.* **34**, 3731-6 (1995).
66. Lee, C., Graves, D. B. , and Lieberman, M. A., *Plasma Chem. and Plasma Proc.* **16**, 99-120 (1996).
67. Hoekstra, R. J., Grapperhaus, M. J., and Kushner, M. J., *J. Vac. Sci. Technol. A* **15**, 1913-21 (1997).
68. Tuda, M., Nishikawa, K., and Ono, K., *J. Appl. Phys.* **81**, 960-7 (1997).
69. Banjo, T., Tsuchihashi, M., Hanazaki, M., Tuda, M., and Ono, K., *Jpn. J. Appl. Phys.* **36**, 4824-8 (1997).
70. Kazumi, H., Hamasaki, H., and Tago, K., *Jpn. J. Appl. Phys.* **36**, 4829-37 (1997).
71. Meeks, E., Ho, P., Ting, A., and R. J. Buss, submitted to *J. Vac. Sci. Technol. A.* (1998).
72. Fleddermann, C. B., and Hebner, G. A., *J. Vac. Sci. Technol. A* **15**, 1955-62 (1997).
73. Hebner, G. A., Fleddermann, C. B. and Miller, P. A., *J. Vac. Sci. Technol. A* **15**, 2698-708 (1997).
74. Tachi, S., Izawa, M., Tsujimoto, K., Kure, T., Kofuji, N., Suzuki, K., Hamasaki, R., and Kojima, M., *J. Vac. Sci. Technol.A.* **16**, 265-9 (1998).
75. Bell, F. H., Joubert, O., Oehrlein, G. S. Zhang, Y., and Vender, D., *J. Vac. Sci. Technol. A* **12**, 3095-101 (1997).
76. Marra, D. C., and Aydil, E. S., *J. Vac. Sci. Technol. A* **15**, 2508-17 (1997).
77. Den, S., Kuno, T., Ito, M., Hori, M., Goto, T., O'Keeffe, P. Hayashi, Y., and Sakamoto, Y., *J. Vac. Sci. Technol. A* **15**, 2880-4 (1997).
78. Rueger, N. R., Beulens, J. J., Schaepkens, M., Doemling, M. F., Mirza, J. M., Standaert, T. E. F. M., and Oehrlein, G. S. *J. Vac. Sci. Technol. A* **15**, 1881-9 (1997).
79. Bjorkman, C. H., Shan, H., Doan, K., Wang, J., Pu, B., and Welch, M., "Effect of hydrogen in high aspect ratio, small feature dielectric etch", presented at the

American Vacuum Society 44th National Symposium, October 1997, *Book of Abstracts*, p. 149.
80. Standaert, T. E. F. M., Schaepkens, M., Rueger, N. R., Sebel, P. G. M., Oehrlein, G. S., and Cook, J. M., *J. Vac. Sci. Technol.A.* **16**, 239-49 (1998).
81. Stoffels, W. W., Stoffels, E., and Tachibana, K., *J. Vac. Sci. Technol.A.* **16**, 87-95 (1998).
82. Inayoshi, M., Ito, M., Hori, M., Goto, T., and Hiramatsu, M., *J. Vac. Sci. Technol.A.* **16**, 233-8 (1998).
83. Sugai, H., Mitsuoka, Y., and Toyoda, H., *J. Vac. Sci. Technol.A.* **16**, 290-3 (1998).
84. Meeks, E., Larson, R. S., Vosen, S. R., and Shon, J. W., *J. Electrochem. Soc.* **144**, 357-66 (1997).
85. Matsuo, P. J., Kastenmeier, B. E. E., Beulens, J. J., and Oehrlein, G. S., *J. Vac. Sci. Technol. A* **15**, 1801-13 (1997).
86. Brooks, C. B., Buie, M. J., and Vaidya, K. J., *J. Vac. Sci. Technol.A.* **16**, 260-4 (1998).
87. Graves, D. B., Kushner, M. J., Gallagher, J. W., Garscadden, A., Oehrlein, G. S., and Phelps, A. V., "Database Needs for Modeling and Simulation of Plasma Processing", National Academy Press, Washington, DC, 1996.
88. Christophorou, L. G., Olthoff, J. K., and Rao, M. V. V. S., *J. Phys. Chem. Ref. Data* **25**, 1341-88 (1996); **26**, 1-15 (1997); **26**, 1205-37 (1997); **28**, 1-29 (1998).
89. Morgan, W. L., *Kinema Research Web Site*, http://www.csn.net/kinema.
90. Oehrlein, *Surf. Sci.* **386**, 222-30 (1997).
91. Penetrante, B. M., Hsiao, M. C., Bardsley, J. N., Merritt, B. T., Vogtlin, G. E., Kuthi, A., Burkhart, C. P., and Bayless, J. R., *J. Adv. Oxid. Technol.* **2**, 299-305 (1997).
92. Penetrante, B. M., Hsiao, M. C., Bardsley J. N., Merritt, B. T., Vogtlin, G. E., Wallman, P. H., Kuthi, A., Burkhart C. P., and Bayless, J. R., "Power consumption and byproducts in electron beam and electrical discharge processing of volatile organic compounds", in *Proceedings of the 2nd Int. Symp. on Environmental Applications of Advanced Oxidation Technologies*, San Francisco, February 1996 (Electrical Power Research Institute), pp. 5-74 to 5-88.
93. Penetrante, B. M., Bardsley, J. N., and Hsiao, M. C., *Jpn. J. Appl. Phys.* **36**, 5007-17 (1997).
94. Itikawa, Y., Hayashi, M., Ichimura, A., Onda, K., Sakimoto, K., Takayanagi, K., Nakamura, M., Nishimura, H., and Takayanagi, T., *J. Phys. Chem. Ref. Data* **15**, 985-1010 (1986).
95. Majeed, T., and Strickland, D. J., *J. Phys. Chem. Ref. Data* **26**, 335-50 (1997).
96. Winters, H. F., *J. Chem. Phys.* **44**, 1472-6 (1966).
97. Cosby, P., *J. Chem. Phys.* **98**, 9544-53 (1993).
98. Schofield, *J. Phys. & Chem. Ref. Data,* **8**, 723-98 (1979).
99. Atkinson, R., Baulch, D. L., Cox, R. A., Hampson, R. F., Kerr, J. A., Rossi, M. J., and Troe, J., *J. Phys. Chem. Ref. Data* **26**, 521-1011 (1997).

100. Atkinson, R., Baulch, D. L., Cox, R. A., Hampson, R. F., Kerr, J. A., Rossi, M. J., and Troe, J., *J. Phys. Chem. Ref. Data* **26**, 1329-1499 (1997).
101. Guerra, V., Pinheiro, M. J., Gordiets, B. F., Loureira, J., and Ferreira, C. M., *Plasma Sources Sci. Technol.* **6**, 220-30 (1997).
102. Slavik, J. and Colonna, G., *Plasma Chem. Plasma Proc.* **17**, 305-14 (1997).
103. Vitello, P. A., Penetrante, B. M. and Bardsley, J. N., *Phys. Rev. E* **49**, 5574-98 (1994).
104. Morrow, R., and Lowke, J. J., *J.Phys. D.* **30**, 614-27 (1997).
105. Falkenstein , Z., and Coogan, J. J., *J.Phys. D.* **30**, 817-25 (1997).
106. Naidis, G. V., *J.Phys. D.* **30**, 1214-8 (1997).
107. Kulikovsky, A. A., *IEEE Trans. Plasma Sci.* **25**, 439-46 (1997).
108. Nilsson, J. O., and Eninger, J. O., *IEEE Trans. Plasma Sci.* **25**, 73-82 (1997).
109. Kitayama, J., and Kuzumoto, M., *J.Phys. D.* **30**, 2453-61 (1997).
110. Chang, J. S., Looy, P. C., Arquilla, M., Kamiya, I., and Sinjo, R., *J. Adv. Oxid. Technol.* **2**, 274-7 (1997).
111. Penetrante, B. M., Hsiao, M. C., Bardsley, J. N., Merritt, B. T., Vogtlin, G. E., Kuthi, A., Burkhart, C. P., and Bayless, J. R., *Plasma Sources Sci. Technol.* **6**, 251-9 (1997).
112. Matzing, H., *Adv. Chem. Phys.* **80**, 315-9 (1991).
113. Tas, M. A., van Veldhuizen, E. M., and Rutgers, W. R., *J.Phys. D.* **30**, 1636-45 (1997).
114. Penetrante, B. M., Hsiao, M. C., Merritt, B. T., Vogtlin, G. E., and Wallman, P. H., *IEEE Trans. Plasma Sci.* **23**, 679-87 (1995).
115. Penetrante, B. M., Hsiao, M. C., Merritt, B. T., Vogtlin, G. E., and Wallman, P. H., Neiger, M., Wolf, O., Hammer, T., and Broer, S., *Appl. Phys. Lett.* **68**, 3719-22 (1996).
116. Tas, M. A., van Hardeveld, R., and van Veldhuizen, E. M., *Plasma Chem. Plasma Proc.* **17**, 371-91 (1997).
117. Mizuno, A., Shimizu, K., Mastuoka, T and Furuta, S., *IEEE Trans. Ind. Applicat.*, **31**, 1463-7 (1995).
118. Dinelli, G., Civitano, L., and Rea, M., *IEEE Trans. Ind. Applicat.*, **26**, 535-41 (1995).
119. Song, Y. H., Shin, W. H., Choi, Y. S., and Kim, S. J., *J. Adv. Oxid. Technol.* **2**, 268-73 (1997).
120. Urashima, K., Chang, J. S., and Ito, T., *J. Adv. Oxid. Technol.* **2**, 286-92 (1997).
121. Vercammen, K. L. L., Berezin, A. A., Lox, F., and Chang, J.-S., *J. Adv. Oxid. Technol.* **2**, 312-329 (1997).
122. Penetrante, B. M., Hsiao, M. C., Bardsley, J. N., Merritt, B. T., Vogtlin, G. E., Kuthi, A., Burkhart, C. P., and Bayless, J. R., *Phys. Lett. A* **235**, 76-82 (1997).
123. Penetrante, B. M., Hsiao, M. C., Bardsley, J. N., Merritt, B. T., Vogtlin, G. E., Wallman, P. H., Kuthi, A., Burkhart, C. P., and Bayless, J. R., *Pure Appl. Chem.* **68**, 1083-7 (1997).

124. Hsiao, M. C., Merritt, B. T., Penetrante, B. M., Vogtlin, G. E., and Wallman, P. H., *J. Appl. Phys.* **78**, 3451-6 (1995).
125. Penetrante, B. M., Hsiao, M. C., Bardsley, J. N., Merritt, B. T., Vogtlin, G. E., Wallman, P. H., Kuthi, A., Burkhart, C. P., and Bayless, J. R., *Phys. Lett. A* **209**, 69-77 (1995).
126. Bromberg, L., Cohn, D. R. , Koch, M., Patrick, R. M., and Thomas, P., *Phys. Lett. A* **173**, 293-9. (1993).
127. Koch, M., Cohn, D. R., Patrick, R. M., Schuetze, M. P., Bromberg, L., Reilly, D., and Thomas, P. , *Phys. Letter A* **184**, 109-13 (1993).
128. Falkenstein, Z., *J. Adv. Oxid. Technol.* **2**, 223-38 (1997).
129. Vitale, S. A., Hadidi, K., Cohn, D. R., and Falkos, P., *Plasma Chem. Plasma Proc.* **17**, 59-91 (1997).
130. Chang, J. S., Yamamoto, T., Kohno, H., Tamura, M., Honda, S., Shibuya, A., and Berezin, A. A., *J. Adv. Oxid. Technol.* **2**, 346-52 (1997).
131. Zipf, E. C., *J. Geophys. Res.* **85**, 687-94 (1980).
132. Burch, R., *Pure Appl. Chem.* B68, 377-85 (1996).
133. Tonkyn, R., Barlow, S., Orlando, T., "Destruction of chlorinated hydrocarbons in a packed bed corona reactor" *Abstracts of the World Environmental Congress,* London, Ontario, September 1995, p. 214.
134. Prieto, G., Prieto, O., Gay, C. R., Mizuno, K., Tamori, I., and Yamamoto, T., *J. Adv. Oxid. Technol.* **2**, 330-6 (1997).
135. Kinoshita, K., Watanabe, S., Hayashi, N., Uchida, Y., Dykes, D., and Touchard, G., *J. Adv. Oxid. Technol.* **2**, 278-82 (1997).
136. Atkinson, R., *J. Phys. Chem. Ref. Data* **26**, 215-290 (1997).
137. Collison, W. Z., Ni, T. Q., and Barnes, M.S., *J. Vac. Sci. Technol.A.* **16**, 100-7 (1998).
138. Woodworth, J. R., Riley, M. E., Miller, P. A., Nichols, C. A., and Hamilton, T. W., *J. Vac. Sci. Technol. A.* **15**, 3015-23 (1997).
139. Hopwood, J., *Plasma Sources Sci. Technol.* **1**, 109 (1992).
140. Patrick. R., Schoenborn, R., and Toda, H., *J. Vac. Sci. Technol. A.* **11**, 1296 (1993).
141. Donnelly, V. M., *J. Appl. Phys.* **79**, 4597 (1992).
142. Gaddy, G. A., Webb., S. F., and Blumenthal, R., *Appl. Phys. Lett.* **71**, 3206-8 (1997).
143. Tokunaga, O., Suzuki, N., Nishimura, K, and Washino, M., *Int. J. Appl. Rad. Isotopes* **29**, 81 (1978).